Fall 2016

Correlation anaylsis of magnesite dissolution rate and magnesite spatial distribution

Yao Wang

Department:

CORRELATION ANALYSIS OF MAGNESITE DISSOLUTION RATE AND MAGNESITE SPATIAL DISTRIBUTION

by

YAO WANG

A THESIS

Presented to the Faculty of the Graduate School of the

MISSOURI UNIVERSITY OF SCIENCE AND TECHNOLOGY

In Partial Fulfillment of the Requirements for the Degree

MASTER OF SCIENCE IN PETROLEUM ENGINEERING

2016

Approved by

Dr. Peyman Heidari, Advisor
Dr. Baojun Bai
Dr. Mingzhen Wei

ABSTRACT

This thesis presents a correlation analysis of the spatial distribution and permeability of magnesite dissolution and focuses on its overall rate and average porosity. Magnesite dissolution is affected by several aspects.

A reservoir's large spatial distribution can make capturing the magnesite dissolution difficult, so in this study, a variogram was built in Petrel using a percentage variation of magnesite and sand. The variogram also handles different major and minor directions in anisotropy. After building the magnesite model, simulation of magnesite dissolution was achieved in Cruch Flow to get the magnesite dissolution rate and average porosity.

For correlation analysis, a regression model was used to build a linear relationship in the correlation analysis. Areas of study included major anisotropy, permeability, minor anisotropy, and percentage of magnesite with dissolution rate and average porosity. The mean of all data was calculated with 95% confidence intervals, and the original data were judged at almost normal value. Finally, correlation analysis included all independent variance with dissolution rate and average porosity.

From all analysis, can find the most important parameter is the percentage of magnesite and sand, next is the major and minor anisotropy, and permeability of magnesite and sand weakest. For a percentage of magnesite has positive correlation with overall rate and average porosity, major anisotropy and permeability have a positive correlation with overall rate and negative correlation with porosity, minor anisotropy has both negative correlation with rate and porosity.

ACKNOWLEDGMENTS

I would like to express my sincere gratitude to my advisor, Dr. Peyman Heidari, for his guidance, patience, and support. I could not reach to anything without his continuous support. It has been an honor to be his student. I would also like to thank my committee members Dr. Baojun Bai and Dr. Mingzhen Wei.

Also, I want to send my appreciation to all of my colleagues: Hasan Al-Saedi, Hector Donoso, Mahta Ansari, Kelsi Leverett, Sameer Salasakar, and Pu Han for their help and teamwork.

Finally, I would like to thanks my parents, they are always supporting me and encouraging me.

TABLE OF CONTENTS

Page

LIST OF ILLUSTRATIONS

Page

LIST OF TABLES

Page

NOMENCLATURE

Symbol	Description
k_1, k_2, k_3	Reaction rate constants for magnesite dissolution (mol/m2/s)
IAP	Ion activity product
K_{eq}	Equilibrium constant
R_{MgCO_3}	Dissolution rate of magnesite (mol/s)
R_f	Forward direction of dissolution rate
$\emptyset_{avg}$	Average porosity
V_{Mg}	Total volume of magnesite
$\bar{X}$	Mean of data
P_i	Probability the values of X takes x_i
$C(\vec{L})$	Theoretical covariance
σ	Standard deviation
σ^2	Variance
$\gamma(h)$	Semivariogram
α_{max}	Major range of the anisotropy
α_{min}	Minor range of the anisotropy
β_1	Coefficients
v	Flow velocity (m/d)

1. INTRODUCTION

Mineral dissolution is a widespread phenomenon. It can lead to changing reservoir properties during mineral dissolution reaction. It can also affect the chemical on fluid-rock-gas interaction (Hamzaoui-Azaza, Ketata et al. 2011, Zhu, Murali et al. 2011). Although magnesite dissolution is not as common as calcite and dolomite dissolution (Chou, Garrels et al. 1989), it is important for understanding the earth system formation.

Magnesite dissolution rate in laboratory and field has a big difference. Mainly reasons lead to this result is we cannot capture the effect of surface area and pore media of heterogeneity. Minerals generated in nature, so minerals have a various spatial pattern. Because grain size is different in a different area, and the complexity of the natural pore media itself on reaction rate and transport (Schott, Brantley et al. 1989), so the effect of surface area is difficult to capture up.

From studies, we knew spatial distribution influences heterogeneity (Li, Li et al. 2007, Molins, Trebotich et al. 2012). Magnesite dissolution heterogeneity will either be physical or chemical. Physical heterogeneity is usually due to flow and transport processes (Gronowitz, Mellström et al. 2006, Li, Peters et al. 2007). Chemical heterogeneity is due to mineral's spatially difference in porous media.

To getting more information about magnesite dissolution, using simulation is very effective. However, magnesite dissolution also has a number of characteristics such as pH value, temperature, porosity, and permeability, which can influence the dissolution rate.

This thesis is focused on correlation analysis between spatial distribution and permeability with magnesite dissolution overall rate and average porosity. A natural reservoir has a large amount of spatial distribution, which cannot be captured. However,

simulation allows us to show magnesite dissolution in a natural reservoir. A variogram was built in Petrel to determine variations in magnesite and sand percentages. The variogram also dealt with different major and minor direction anisotropy. Then simulation shows magnesite dissolution in Crunch Flow. For discussing the linear relationship between spatial distributions and permeability with the magnesite dissolution overall rate and average porosity, we built a regression model for global sensitivity analysis. The spatial distribution uses a variogram reservoir, and permeability was determined according to different levels of magnesite and sand.

2. LITERATURE REVIEW

2.1. MAGNESITE DISSOLUTION

Minerals dissolution: The minerals dissolution refers to chemical processes; it's important for understanding the earth system formation and its aspects such as atmospheric chemistry, soil, and the environment. Mineral dissolution reactions have been widely investigated in laboratory work and in the field. The Figure 2.1. shows calcite dissolution at different times in the same area at 25 °C. Mineral dissolution reactions can change reservoir properties.

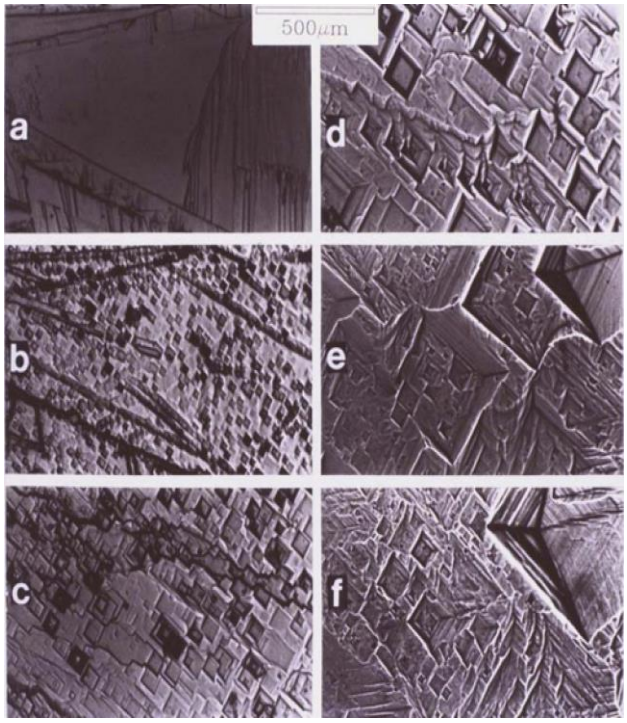

Figure 2.1. Photomicrographs of calcite dissolution of the same area at 25° C, after (a) 0 h, (b) 0.5 h, (c) 1.5 h, (d) 3 h, (e) 11 h, and (f) 17.5 h total dissolution time (Brantley, Bandstra et al. 2008)

Minerals dissolution studies began in the late 19^{th} century. Boguski was the first to show the rate of marble solution as proportional to the molar concentration of acid used as solute (Boguski 1876). His research was followed by research dedicated to linking the dissolution rate with diffusion theory. In the 1920's, scientists found that the carbonic acid diffusion rate on marble surfaces influences dissolution rates. The diffusion rate was also found to be dependent on pH value (Faurholt 1924). After that, researchers began looking for relationships between saturation parameter, viscosity of solute, and diffusion rate with dissolution rate.

In the 1960s, Berner proposed ion activity products (IAP'S). The quoted study experimentally identified IAP in calcite and dolomite. Studies in the 1970s defined more parameters such as pH range, temperature, and overall reaction.

In 1976, Plummer et al. mentioned an equation of dissolution rate, and it has been widely utilized. The dissolution rate was expressed as(Plummer and Wigley 1976):

$$R_f = k_1 * a_H + k_2 * a_{H_2CO_3} + k_3 * a_{H_2O} \quad (1)$$

Where R_f stands for forward direction of dissolution rate, $k_1, k_2,$ and k_3 are rate constants, a_i activity of the subscript species.

Afterwards, scientists focused on the flow through porous media model and development of reactive flow modeling (Murphy and Cummins 1989). This model is for steady-state flow with one dimensional, one component and homogeneous systems.

However, homogeneous systems are idealized theoretical systems and are actually nonexistent in the reservoir. Hence, investigation of natural reservoir's homogeneity has been approached on different scales (Bagheri and Settari 2006).

During the past decade, studies have focused on spatial heterogeneity of mineral dissolution, such as flow velocity, reaction scale, and spatial distribution.

Magnesite dissolution in Laboratory and field studies: Now a great number of magnesite studies occur (Figure 2.2. SEM image of magnesite ore) attaining dissolution rates in laboratory and field. In total, the laboratory dissolution work's magnitude is greater than that observed in the field with a ratio of two to five (White and Brantley 2003, Maher 2010, Lüttge, Arvidson et al. 2013, Reeves and Rothman 2013).

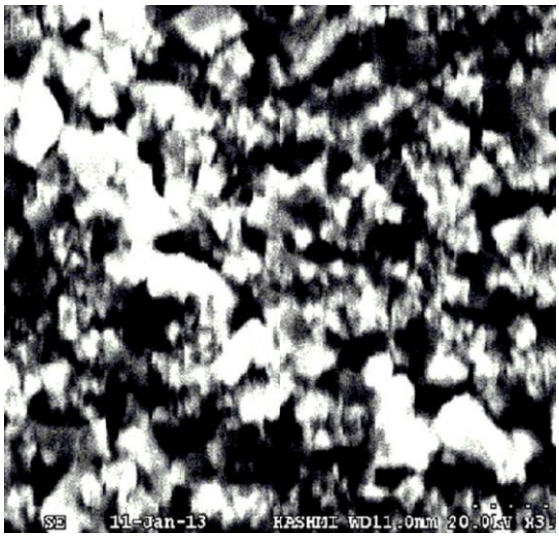

Figure 2.2 SEM photomicrographs of natural magnesite ore (Raza and Zafar 2013)

Major differences between lab and field studies have to do with secondary mineral precipitation (Alekseyev, Medvedeva et al. 1997, Nugent, Brantley et al. 1998); effect of surface area in dissolution reactions (Swoboda-Colberg and Drever 1993), and residence

time of fluid (Maher 2010). Of these three areas of study, surface area dissolution reactions are usually the most valued.

When all conditions of laboratory and field are the same, laboratory magnesite dissolution rate will be 200~400 times faster than that in the field (Swoboda-Colberg and Drever 1993). In the past several years, scholars have used the AFM method to find the effect of surface area dissolution reactions and dissolution rate (Levenson 2013). Other studies proposed dissolution rate is influenced by the pore media of physical and chemical heterogeneity (Li, Peters et al. 2007, Molins, Trebotich et al. 2012).

The reactive surface area is easy to understand, but it is difficult to assess because numerous factors affect it, such as mineral's heterogeneity distribution and the age of minerals. In nature, the pore media mainly depends on the spatial distribution of minerals, the grain size of different areas, and the complexity of the natural pore media itself on reaction rate and transport (Devidal, Schott et al. 1997, Liu and Dreybrod 1997).

Other researchers revealed that the concentration of fluid can influence the reactive surface area. This is because the effect of surface area decreases with the equilibration fluid through the pores. The reason for the decrease in the effectiveness of the surface at equilibrium conditions is that some of the pores do not take part in the reaction (Brantley, Bandstra et al. 2008).

Magnesite dissolution rate: Mineral dissolution applies to a mass of minerals such as dolomite, calcite, and aragonite. (Chou, Garrels et al. 1989) Magnesite dissolution is mineral dissolution. Numerous carbonate models have mentioned dissolution in acidic solution (Plummer and Wigley 1976, Sjöberg and Rickard 1984, Pokrovsky, Schott et al. 1999). The magnesite dissolution is always occurring on the solid and water interface and

has three parallel reactions (Plummer, Wigley et al. 1978, Chou, Garrels et al. 1989, Wollast 1990):

$$MgCO_3 + H^+ \leftrightarrow Mg^{2+} + HCO_3{}^- \quad (2)$$

$$MgCO_3 + H_2CO_3 \leftrightarrow Mg^{2+} + CO_3{}^{2-} \quad (3)$$

$$MgCO_3 \leftrightarrow Mg^{2+} + CO_3{}^{2-} \quad (4)$$

Magnesite dissolution and crystallization rate are described by (Pokrovsky, Schott et al. 1999):

$$R_{MgCO_3} = k_1 * a_{H^+} + k_2 * a_{H_2CO_3} + k_3 - k_3 * a_{Mg^{2+}} * a_{CO_3{}^{2-}} \quad (5)$$

According to Transition State Theory (TST), the magnesite dissolution rate also can be expressed as (Li, Salehikhoo et al. 2014):

$$R_{MgCO_3} = \left(k_1 * a_{H^+} + k_2 * a_{H_2CO_3} + k_3\right) * A * \left(1 - \frac{IAP}{K_{eq}}\right) \quad (6)$$

$$IAP_{MgCO_3} = a_{Mg^{2+}} * a_{CO_3{}^{2-}} \quad (7)$$

where R represents the overall rate for magnesite, and k_i are the rate constants of reactions (2)-(4), the unit is mol/m^2/s; and a_i stands for the activities of aqueous species. A is the magnesite surface area, and the unit is $m^2/\ m^3$ pore volume. IAP is the ion activity product of Eq. (4) $a_{Mg^{2+}}$and$a_{CO_3{}^{2-}}$, which is in (7). K_{eq} stands for equilibrium constant, which is also used to describe Eq. (4). So the $\frac{IAP}{K_{eq}}$ represents the distance from equilibrium. The value of the $\frac{IAP}{K_{eq}}$ between one and zero: at the beginning it is near to zero, and one is the function closest to equilibrium.

Heterogeneity: In natural porous media, such as that found in oil and gas reservoirs, soil, and in the earth's crust, heterogeneity refers to their common characteristics and is

categorized into three types: chemical, physical, and microbial. For magnesite dissolution, we focused on chemical and physical heterogeneity.

Physical heterogeneity is influenced by porous media of spatial distribution, such as some physical properties: density, porosity, and permeability. A number of areas use physical heterogeneity, as in the case of enhanced oil recovery for petroleum reservoirs (Liu and Dreybrod 1997, Smith, Smith et al. 2005), and modeling of contaminant transport (Mousavi-Avval, Rafiee et al. 2011).

Research has documented the flow velocity that can influence overall dissolution rates. Although at the same mineral spatial distribution, the flow has different overall dissolution rates due to different flow rates in the physical environment (Li, Peters et al. 2007). For example, the intermediate flow regime usually has the lowest overall dissolution rates because this regime manages both reaction and transport.

For chemical heterogeneity, we must consider mineral's spatial difference in porous media. The variation of minerals has a different spatial distribution in the subsurface. In most papers, mineral dissolution rate separates into a different part when well mixed with no heterogeneity. But recent studies using the modeling approach have minerals dissolve when exposed to chemical heterogeneity (Li, Peters et al. 2007, Molins, Trebotich et al. 2012).

In those studies, with variation spatial scales, the overall dissolution rate is different. Figure 2.3. shows different heterogeneity where from left to right, the heterogeneity increases. So the different results in the mineral dissolution overall rate and the local reaction rate is due to different spatial distribution reaction products.

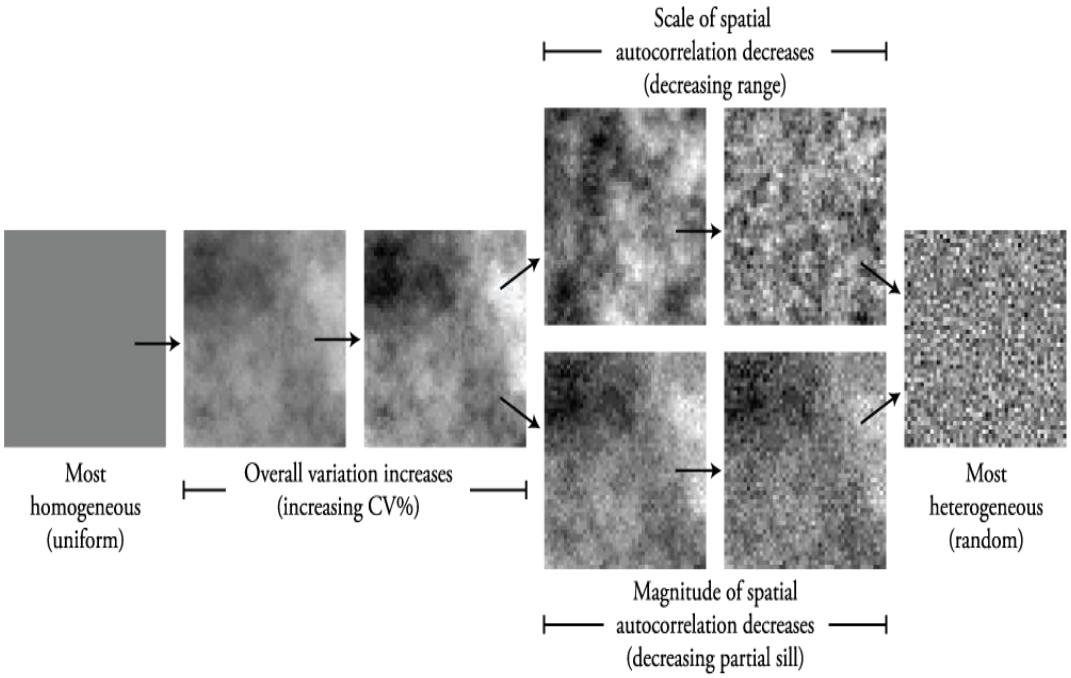

Figure 2.3. Three different types of heterogeneity (Darrouzet-Nardi 2010)

Factors affecting magnesite dissolution rate: For steady-state magnesite dissolution, the ambient temperature is 25℃, and the pH value is between 0.2 to 12 (Lyuksyutov and Pokrovsky 1998, Pokrovsky 1998). When the pH value is lower than 5 it has a linear function with the magnesite dissolution rate (Chou, Garrels et al. 1989)in Figure 2.4., and the reaction rate of Eq. (4) is larger than reaction rate of Eqs (5) and (6). The pH value is higher than 5, and the reaction rate of Eq. (4) is smaller than the reaction rate of Eq. (5) and (6).

Lots of factors affect the magnesite dissolution rate such as pH value, temperatures, and P_{co_2}(Chou, Garrels et al. 1989). Spatial distribution, flow velocity, and porosity has always been able to influence dissolution (Salehikhoo, Li et al. 2013, Li, Salehikhoo et al. 2014). Spatial distribution is important. For instance, in the experiment result testing the

magnesite dissolution rate, the mix column was 14% higher than the one-zone column (Salehikhoo, Li et al. 2013) in Figure 2.5.

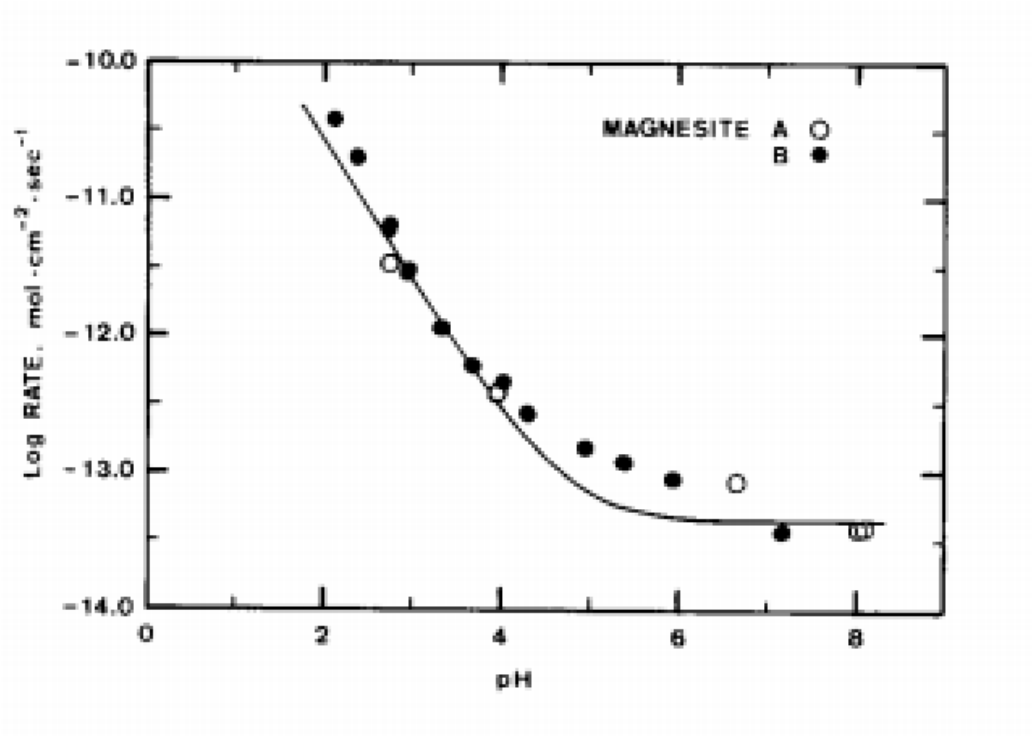

Figure 2.4 Magnesite log (rate) vs. pH and the curve is calculated without the influence ofP_{co_2}. Magnesite B is $MgCO_3$ (Chou, Garrels et al. 1989)

Excluding spatial distribution, other factors can affect the magnesite's average porosity and permeable dispersivty. For example, the average porosity is the ratio of the sum of magnesite pore volume and another mineral's pore volumn. If we have magnesite and quartz, the volume fraction of magnesite is higher with the average porosity$\emptyset_{avg}$. (Li, Salehikhoo et al. 2014) The function is follows:

$$\emptyset_{avg=} \frac{V_{other}*\emptyset_{other}+V_{Mg}*\emptyset_{Mg}}{V_{tot}} \quad (8)$$

In Eq. (8), V_{other} is total volume of the other mineral, and V_{Mg} is the volume of magnesite. The sum of them isV_{tot}. Usually, the porosity of magnesite is equivalent to 0.58.

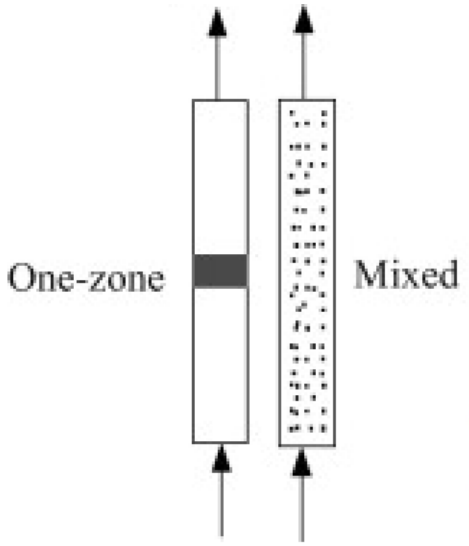

Figure 2.5 Schematic stands for two columns with different spatial distribution. The color of magnesite is black and quartz is white. (Salehikhoo, Li et al. 2013)

2.2. VARIOGRAM

Reservoir heterogeneity: Reservoir heterogeneity is used as a function of space of variation in reservoir properties (Webster and Oliver 1993, Journel and Deutsch 1998, Gringarten and Deutsch 2001, Manto 2005, Bear 2013). The reservoir properties usually contain: permeability, temperature, thickness, and porosity. As usual, we divide reservoir heterogeneity into four types: microscopic heterogeneity used to scale of porous medium;

macroscopic heterogeneity used to scale like core plugs and flow properties; megascopic heterogeneity used to scale the large grain block, also can use in field; gigascopic heterogeneity used to whole reservoir scale (Hewett and Behrens 1990). Figure 2.6 shows the size of all types of reservoir heterogeneity.

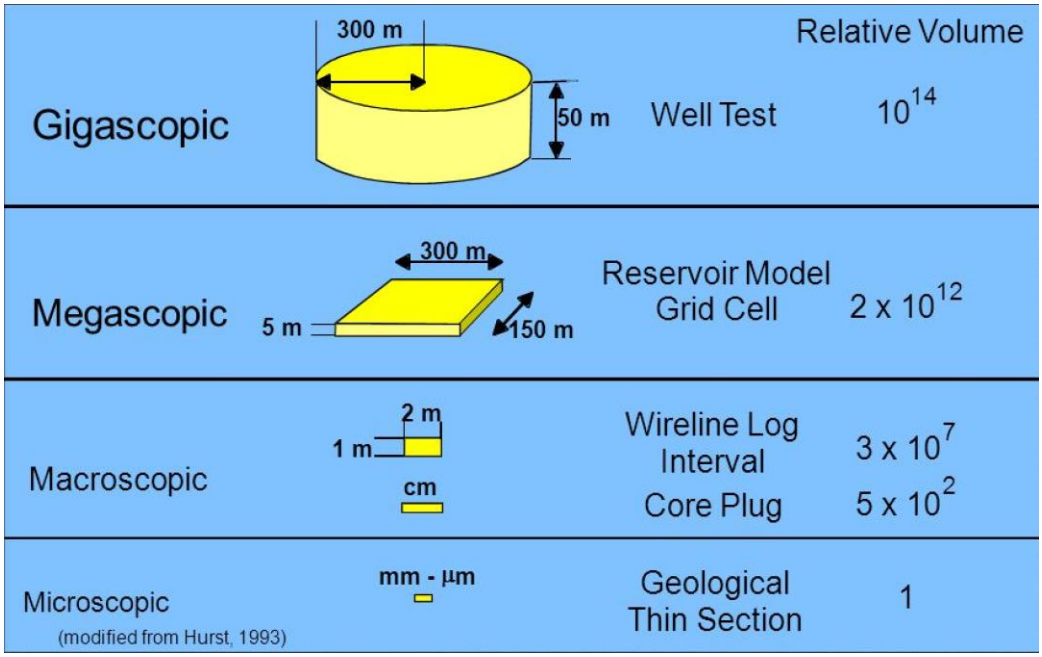

Figure 2.6 The size of four types of reservoir heterogeneity

Most simulations are used at a macroscopic scale. Actually, the macroscopic scale is the porous medium summary of microscopic structure in a continuum (Bear 2013). This study also used the macroscopic scale for modeling.

Geostatistics: Geostatistics is a branch of statistics and a method of description that can summarize the spatial relationship of the variables. It was first used by D.G. Krige in

the South African mining industry (Wackernagel 2013). Matheron developed Krige's method and built a form to analyze and estimate spatial variables.

Nowadays, geostatistics plays a part in several aspects such as interpolation and extrapolation, spatial distribution analysis, risk analysis or uncertainty estimates, and use of intercorrelation attributes (Webster and Oliver 1993, Journel and Deutsch 1998, Wackernagel 2013). For spatial distribution analysis, geostatistics can give us a reservoir property in the spatial variable of the description of the quantitative relationship or the distance between two related variables. In addition, using geostatistics can give us several ways to estimate the value of uncertainties. It also benefits risk anaylsis.

To use geostatistics involves three steps: (1) assumption of stationary, (2) modeling of spatial relationships, (3) estimations. The first step is above all for geostatistic anaylsis, it needs the model build for sample date where the region is stationary. Next step, in total is to build the model of sample data in a spatial relationship. But with distance increasing, the correlationship between data is decreasing. So we use a variogram to define a model using the description of related neighboring data to build a spatial relationship between two variables. Finally, estimation of variables at the unsampled location is achieved, which is also called kriging (Webster and Oliver 1993, Journel and Deutsch 1998, Wackernagel 2013). Because of the different types of estimation, we use different krigings. Furthermore, kriging also can create several reservoir images, each of them with the same probability of existence and they can estimate uncertain relationships.

Geostatistics has lots of advantages. For instance, using sample values infer to the value of unsampled locations, more comprehensively underatanding for sample values, provideing estimation errors for estimation value. But it also has some disadvantage, such

as for analysing needs subjective decision making for each step, it leads to the resluts maybe not objective.

Geostatistic parameters: Geostatistics has a mass of elementary concepts. The most important of those are: mean, variance, expected value, and covariance. The "mean" is the average weight (value or score) of the data. Sometimes the "mean" has a problem, which means it is very easily influenced by outlier data. The equation for a mean value is below (Webster and Oliver 1993, Journel and Deutsch 1998, Wackernagel 2013):

$$\bar{X} = \frac{\sum X}{n} \quad (9)$$

$\bar{X}$ is stans for mean of data, and n is the total number of data, $\sum X$ is equal to sum of all data.

Variance is equal to the square of standard deviation and has the same meaning as standard deviation. The standardized variance is a measure of the distance between the data and the mean. It is very useful and something you read about when making a prediction or another statement about data. The standard deviation (10) equation and equation of variance (11) are written as (Webster and Oliver 1993, Journel and Deutsch 1998, Wackernagel 2013):

$$\sigma = \sqrt{\frac{\sum(X-\bar{X})^2}{(n-1)}} \quad (10)$$

$$\sigma^2 = \frac{\sum(X-\bar{X})^2}{(n-1)} \quad (11)$$

X stands for the score for each point in the data. $\overline{X}$ is the mean of score for the variable; the meaning of $X - \overline{X}$ is the distance from the mean, and n is the sample size.

The expected value is the description of the expected return of the experiment. The equation of expected value follows (Journel and Deutsch 1998, Wackernagel 2013):

$$E(X) = \mu_X = \sum_{i-1}^{n} x_i \times P_i \quad (12)$$

$E(X)$ represents the expected value of X, and is the sum of the values by their respected probability. $P_i = P(X = x_i)$ stands for probability as the value of X takes x_i.

Covariance is used to describe spatial relationships. And for theoretical covariance $\mathrm{C}(\vec{L})$ lies between two random variables $X(\vec{u})$ and $X(\vec{u} + \vec{L})$. If the covariance value is equal to zero, they are uncorrelated. The equation of covariance follows (Webster and Oliver 1993, Journel and Deutsch 1998, Wackernagel 2013):

$$\mathrm{C}(\vec{L}) = \mathrm{C}[X(\vec{u}), X(\vec{u} + \vec{L})] = E[X(\vec{u}), X(\vec{u} + \vec{L})] - E[X(\vec{u} + \vec{L})]E[X(\vec{u})] \quad (13)$$

The values of $X(\vec{u})$ and $X(\vec{u} + \vec{L})$ stand for variables at location $\vec{u}$ and $\vec{u} + \vec{L}$.

Variogram: The variogram is the most common and widely used geostatistical technique; it is used to describe the spatial relationship between values of a parameter. Furthermore, for geostatistical reservoir characterization studies, over 90% are used variogram-based geostatistical methods. In total, the variogram is a description of the expected square difference for two different data values. The beginning variogram is zero, which increases with the lag distance for the two values. The variogram equation follows (Gringarten and Deutsch 2001) (Gringarten and Deutsch 2001):

$$2\gamma(h) = E[Y(u) - Y(u + h)] \quad (14)$$

Y represents a stationary random function; h stands for a distance vector. We can also use a semivariogram $\gamma(h)$, which is half of the variogram $2\gamma(h)$. Figure 2.7 represents the semivariogram. When the distance line in the correlated area continues its upward bound movement until it reaches the sill, where its effective value or practical range can be determined. In this case it corresponds with the variogram and remains almost unchanged.

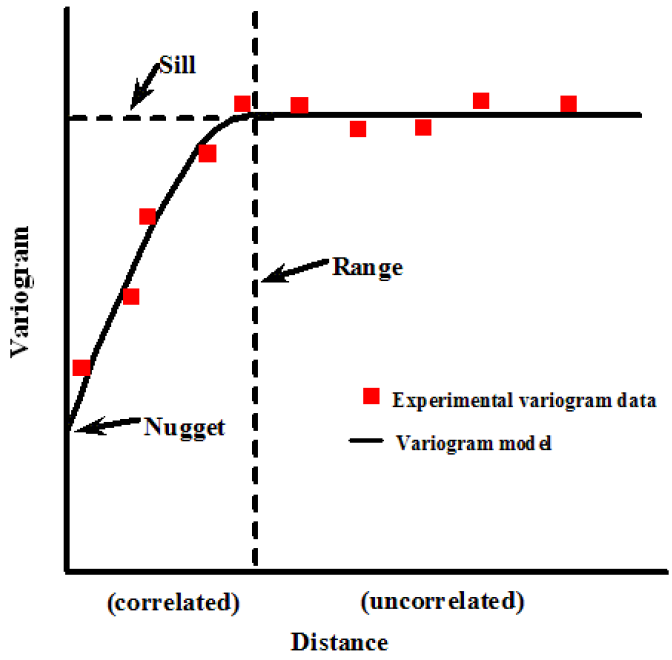

Figure 2.7. Semi-variogram (Journel and Deutsch 1998)

In addition, the covariance and variogram also have a complementary relationship. which must be understood if the variogram is to be properly understood. Eq. (15) establishes some fundamental principles, which were laid down by (Gringarten and Deutsch 2001):

$$\gamma(h) = \mathrm{C}(0) - \mathrm{C}(\mathrm{h}) \quad \text{or} \quad \mathrm{C}(\mathrm{h}) = \mathrm{C}(0) - \gamma(h) \qquad (15)$$

Variogram parameter: The variogram analysis has several parameters, which are important to constructing a variogram and for estimating the autocorrelation structure of the underlying stochastic process. The most popular variogram paradigm usually follows three parameters: sill, range, and nugget effect as shown in Figure 2.8.

The nugget effect (θ_0) is a micro-scale of pure random variation, which is also used to measure error and can usually be found in a state of discontinuity where $\gamma(h)$ at$h = 0$.

Range represents the distance for the semivariogram at a constant and also stands for the distance wherein the data are no longer correlated. Figure 2.8 gives this range as θ_2. The sill (γ_∞) describes the variance of the random field and neglects the spatial structure (Budrikate, 2005).

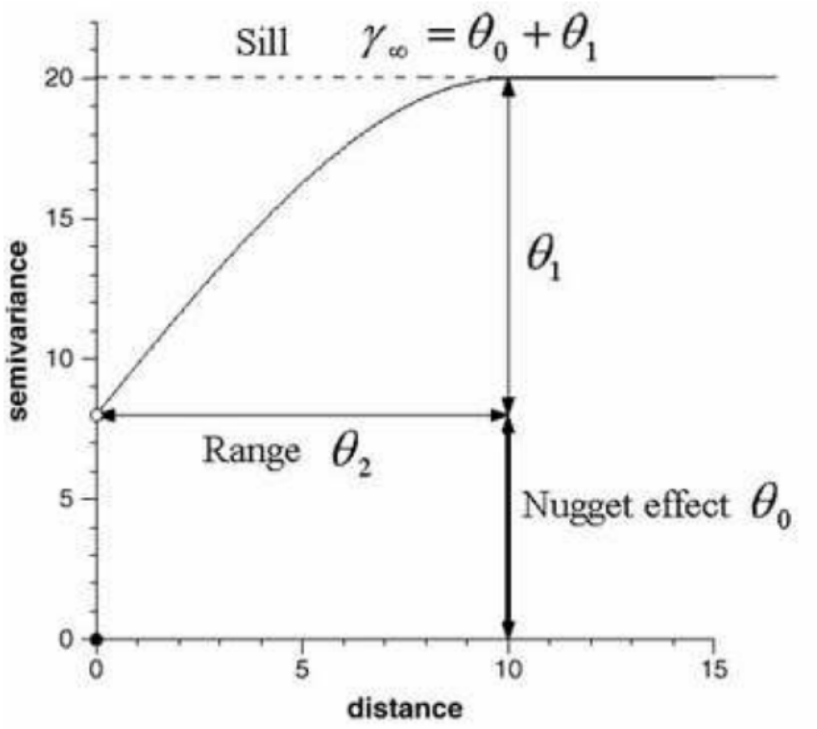

Figure 2.8. Semi-variogram schematiac (Bohling 2005)

Variogram model: The variogram model is one of two types: with sill or without sill. The models with sill contain a spherical model, exponential model, Gaussian model, and nugget model. The models without sill contain a linear model and a power model. The

most commonly studied models are those with sill (Warrick and Myers 1987, Gringarten and Deutsch 2001, Bohling 2005, Bear 2013). Table 2.1 is the equation for five popular models. h represents lag distance, a represents range and c is the sill.

Table 2.1. The equation for five common models (Bohling 2005)

Model type	Equation
Nugget	$g(h) = \begin{cases} 0 \; if \; h = 0 \\ c \quad otherwise \end{cases}$
Spherical	$g(h) = \begin{cases} c * \left[1.5\left(\frac{h}{a}\right) - 0.5\left(\frac{h}{a}\right)^3\right] \; if \; h \leq a \\ c \quad otherwise \end{cases}$
Exponential	$g(h) = c * \left[1 - exp\left(\frac{-3h}{a}\right)\right]$
Gaussian	$g(h) = c * \left[1 - exp\left(\frac{-3h^2}{a^2}\right)\right]$
Power	$g(h) = c * h^{\omega}$ with $0 < \omega < 2$

The spherical model characteristic achieves c, while the specified sill value at a represents a specified range. As for the exponential and Gaussian models, a can reach 95%

of the specified sill value (Journel and Deutsch 1998, Gringarten and Deutsch 2001, Bohling 2005, Bear 2013). At the beginning, the exponential and Gaussian trends are nearly linear. The three types of models are compared in Figure 2.9.

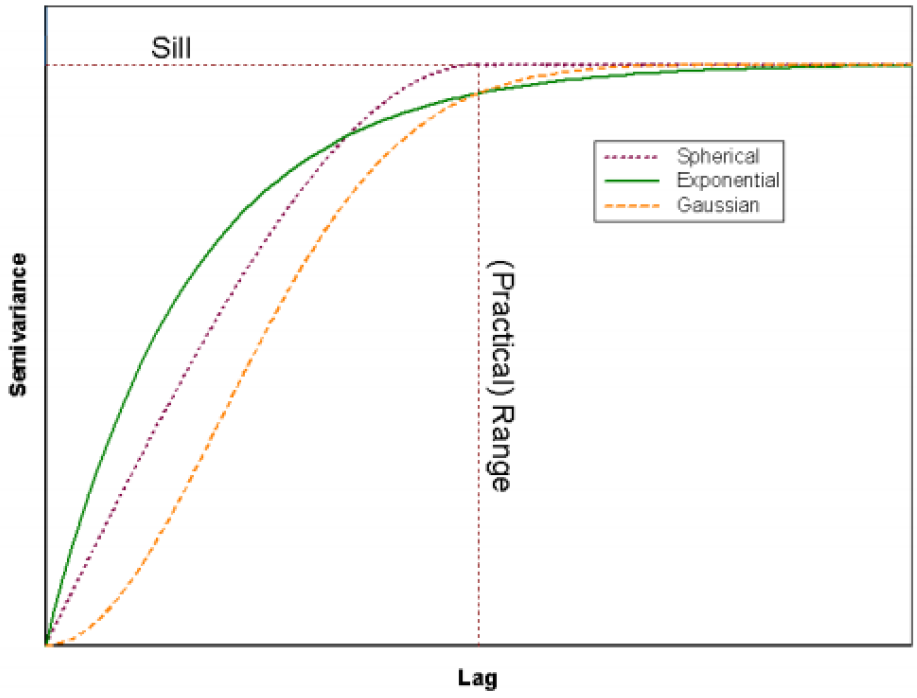

Figure 2.9. Three types of variogram models (Bohling 2005)

Variogram interpretation: The variogram interpretation contains: trend, cyclicity, geometric anisotropy, and zonal anisotropy. For this thesis, the most important variogram interpretation is geometric anisotropy.

The variogram is anisotropic, and for the variogram's two types of anisotropy: geometric anisotropy and zonal anisotropy (Jackson and Caldwell 1993, Journel and

Deutsch 1998, Gringarten and Deutsch 2001, Bear 2013). Geometric anisotropy exists within the range, and at the point shown in Figure 2.10 until it has to change in a different direction. Zonal anisotropy appears for sill to change the direction of the semivariogram.

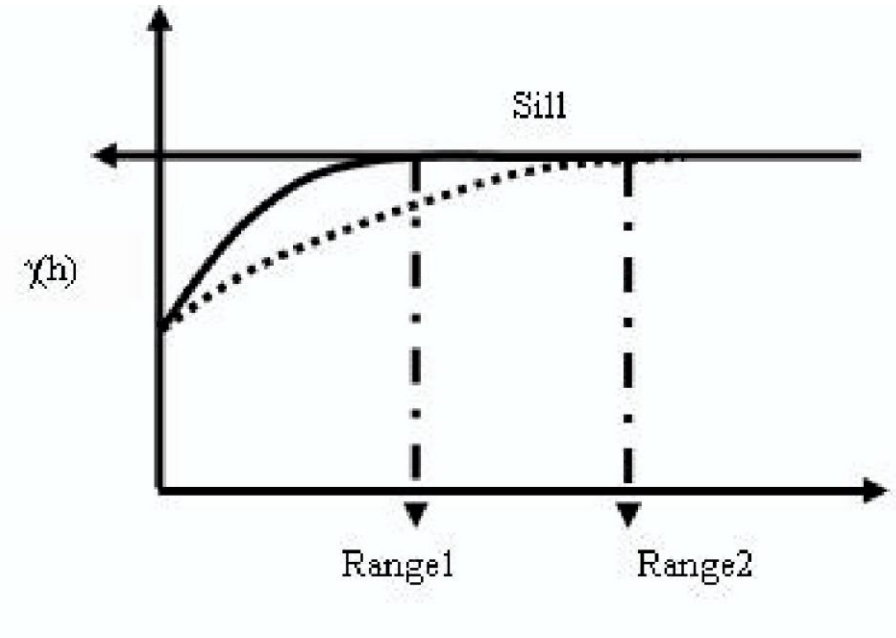

Figure 2.10. Geometric anisotropy (Bohling 2005)

In a word, the geometric anisotropy in one direction correlation is bigger than when it is going in the other direction. In a two-dimensional range of direction, the distance between the center and the edge of the ellipse can be determined mathematically.

The picture of two dimensional geometric anisotropies as shown in Figure 2.11. gives $\alpha_{max}$for ellipse as the major range of the anisotropy, and α_{min} is the minor range of anisotropy (Journel and Deutsch 1998, Gringarten and Deutsch 2001, Bear 2013).

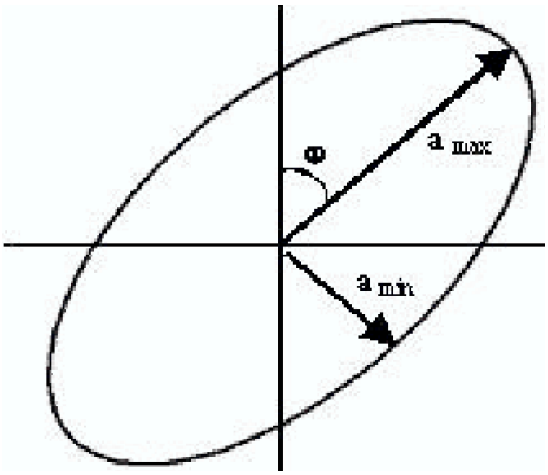

Figure 2.11. Directional ranges: two-dimensional case (Manto 2005)

2.3. GLOBAL SENSITIVITY ANALYSIS

Global sensitivity analysis is a great way to approach data analysis, and it applies to many types of research such as physics, behavioral science, business, and education (Wagner 1995). In the beginning, the methodological structure was simple. Today, we have more and more models to match different variable data. In total, global sensitivity analysis has several methods including eFAST, regression model, and Morris model (Wagner 1995, Saltelli, Ratto et al. 2008). This thesis presents and recommends the use of a regression model to analyze correlation ships.

Regression analysis: For all statistical techniques, linear regression analysis is the most common. The regression model describes the relationship between one dependent variable and one or more independent variables. As usual, the response variable (Y) is a function of one or more driver variables ($X_1, X_2, X_3, \cdots, X_n$) (Draper, Smith et al. 1966, Hair, Black et al. 2006):

$$Y = \beta_0 + \beta_1 X_1 + \beta_2 X_2 + \beta_3 X_3 \cdots \beta_n X_n + \varepsilon \quad (16)$$

$\beta_{1,}\beta_2, \cdots, \beta_n$ as the coefficients also represent the slopeless equation, and ε stands for random error term or residuals, while β_0 represents the Y intercept. Except for ε, the front part is a linear component (Fox 1997).

The regression model always has two types: simple regression and multiple regression. If in regression analysis, only one driver variable is available, which is a simple regression. If the analysis has more than one driver variable and one response variable, it represents multiple regression.

Figure 2.12 shows the variable relationship of the regression model where the first one (left) has a strong positive relationship, the middle one has a strong negative relationship, and the right one has no relationship.

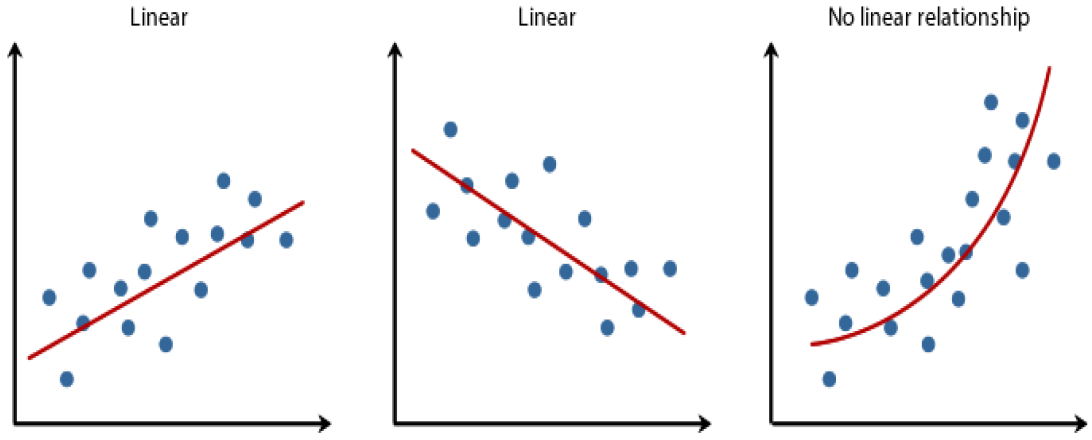

Figure 2.12 Three relationships of regression model (Norusis 2006)

2.4. OBJECTIVE

For magnesite dissolution spatial distribution studies, the laboratory has been a resource that is reliable and convenient, but the laboratory is limited to simulating the real reservoir. Hence, researchers will use protocols involving a variety of zones categorized as a mixed case, one-zone case, and four-zone case to simulate the core-to-magnesite dissolution. In this thesis, we used a Petrel software-derived variogram to simulate magnesite and obtain a great number of cases. In a variogram, we can set different percentages of the magnesites and sand, and we also can set the major or minor anisotropy. By using a variogram we were able to get more information about the spatial distribution influence on magnesite dissolution.

Because we have many different variograms, we can simulate magnesite dissolution. After simulation, we can determine the rate, porosity, and breakthrough. With such a large database, we were able to do lots of analyses.

To analyze the data, we focused on which parameters are sensitive to the overall rate and average porosity? We defined the relationship between parameters and built the regression model to correlation analysis, and found the relation equation between the parameters. We compared them to find what the most important parameter is.

3. METHODOLOGY

3.1. REACTIVE TRANSPORT

In magnesite dissolution lots of aqueous speciation reactions occur; hence, content will vary among the many species, which can include the following::$Mg^{2+}, MgHCO_3{}^-$, $MgCO_3(aq), Cl^-$, $H_2CO_3, HCO_3{}^-, CO_3{}^{2-}, H^+$, OH^-, Na^+, K^+, Br^-. Some reactions are fast and some are slow depending on whether the species initiate the reaction as primary agents or react as secondary agents. In the magnesite dissolution, primary species are:$Mg^{2+}, HCO_3{}^-, H^+, Na^+, K^+, Br^-$. All others are secondary species. For magnesite dissolution, the values of k_1, k_2, k_3 in Eq. (6) are 2.5E-5, 6E-6, and 4.5E-10, respectively (Chou et al., 1989).

3.2. NUMERCIAL SIMULATION

CrunchFlow is a software for simulation, and it used to assist in planning geochemical system transport processes and modeling flow (Steefel and Lasaga 1994; Steefel 2009).

Equations (2), (3), and (4) are used to simulate magnesite dissolution. The initial and inlet conditions for magnesite dissolution are shown in Table 3.1, and the simulation provides a 2D model, sized as 200*200 grid blocks in the X-Y coordinate, as shown in Figure 3.1.

Table 3.1 Initial and inlet conditions

Units	Inlet Condition	Initial conditions
Temperature	25.0	25.0
pH	4.0	8.0
SiO2(aq)	1.0E-9	1.0E-9
CO2(aq)	1.2581E-9	1.2581E-9
Br-	1.00E-4	1.0E-7
Na+	1.0000E-3	1.0000E-3
Ca++	1.2581E-9	1.2581E-9
Cl-	1.0000E-3	1.0000E-3
Mg++	1.2581E-9	1.0E-7

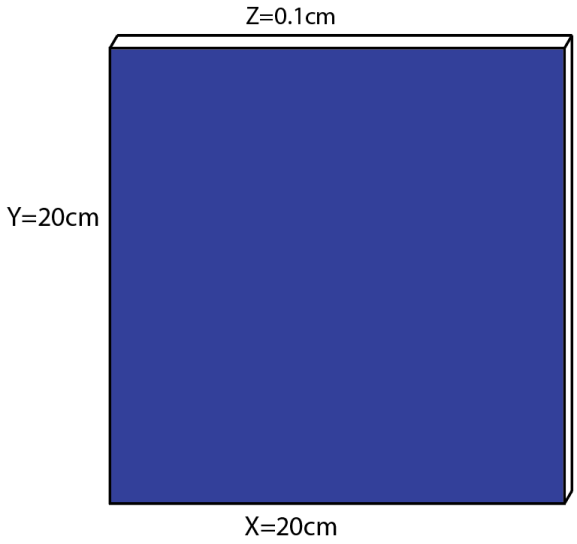

Figure 3.1 Geometry of the model used in the simulation

3.3. VARIOGRAM IN PETREL

The present variogram figure is created by Petrel. Petrel is a reservoir software used to build reservoir models, interpret seismic data, and perform well correlation (Gringarten and Deutsch 2001). For variogram setup, we first set up a method for facies as the sequential indicator simulation (Gslib). Other parameters for the variogram are shown in Table 3.2. Then for the variogram facies set, we used different percentages of magnesite and sand: 90% sand to 10% magnesite, 80% sand to 20% magnesite; 70% sand to 30% magnesite, 60% sand to 40% magnesite, and 50% sand to 50% magnesite.

Table 3.2 Variogram in Petrel parameters

Parameter	Type/values
Size	200mm*200mm*1mm
Sill	1
Nugget	0.0001
Variogram type	Exponential
Anisotropy range in major direction and minor direction	1&1, 10&1, 10&10, 20&1, 20&10, 20&20, 50&1, 50&10, 50&20, 50&50, 100&1, 100&20, 100&50, 100&100
Anisotropy range in vertical direction	2
Major direction orientation for azimuth	0
Major direction orientation for dip	0

The final step was to run the variogram in different anisotropy ranges in major and minor directions 10 times and also run it with different percentages of magnesite and sand. The end result was 750 files for variogram.

3.4. REGRESSION ANALYSIS

For this thesis, the author used MATLAB® to do the multiple linear regression analysis. For regression models, the overall rate and average porosity were selected as dependent variables, and I chose the major anisotropy, minor anisotropy, magnesite percentage at initial interaction, and permeability of sand and magnesite as independent variables.

The workflow is shown in Figure 3.2. For regression analysis, our first need was to convert the data form Excel to MATLAB®. The next step was to delete the invalid data and outlier data. We analyzed the correlation among data and removed the non-correlation data. Finally, we built a regression model and did regression analysis step by step. In the end, can get the figure and equation of regression model.

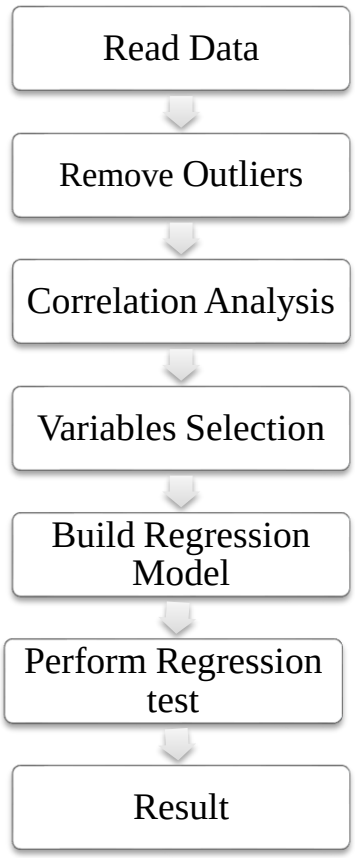

Figure 3.2. Workflow for regression analysis

4. RESULT AND DISCUSSION

4.1. BASIC PARAMETER RESULTS

The basic parameters contents: percentage of magnesite (sand), the permeability of magnesite and sand, the major anisotropy and minor anisotropy. There are very important for analysis magnesite dissolution rate.

4.1.1. Percentage. The percentage of magnesite is an important parameter of dissolution rate. With magnesite percentage increasing, the dissolution rate also is increasing.

The following test called for picking up four cases from 2,250 cases to analyze different percentages of magnesite and sand to determine how the magnesite-to-sand ratio would affect the results of magnesite dissolution. Table 4.1 illustrates the basic condition of the 4 cases.

Figure 4.1 (a)–(d) shows the four cases and the spatial distribution of magnesite and sand. From left to right, the percentage of magnesite increased as the percentage of sand decreased.

Figure 4.1 (e)–(h) show the magnesite dissolution rate, with the black portion of the marker column recording the highest reaction rates. So comparing (e)–(h), left to right, tells us the lower percentage of magnesite had the highest reaction rate, while Figure 4.1 (i)–(l) showed the saturation index of the pore solution.

A value of zero indicates an equilibrium condition. From left to right, the redder the zone the closer the mixture came to equilibrium conditions. So the higher percentage of magnesite had a higher saturation.

Table 4.1. The parameters of the different percentage of magnesite

	Flow rate	Sand permeability	Magnesite permeability	Major Anisotropy	Minor Anisotropy	Magnesite Percentage Initial	Sand Percentage Initial
a	5	1.00E-12	1.00E-13	50	50	0.093475	0.906525
b	5	1.00E-12	1.00E-13	50	50	0.199	0.801
c	5	1.00E-12	1.00E-13	50	50	0.39025	0.60975
d	5	1.00E-12	1.00E-13	50	50	0.5021	0.4979

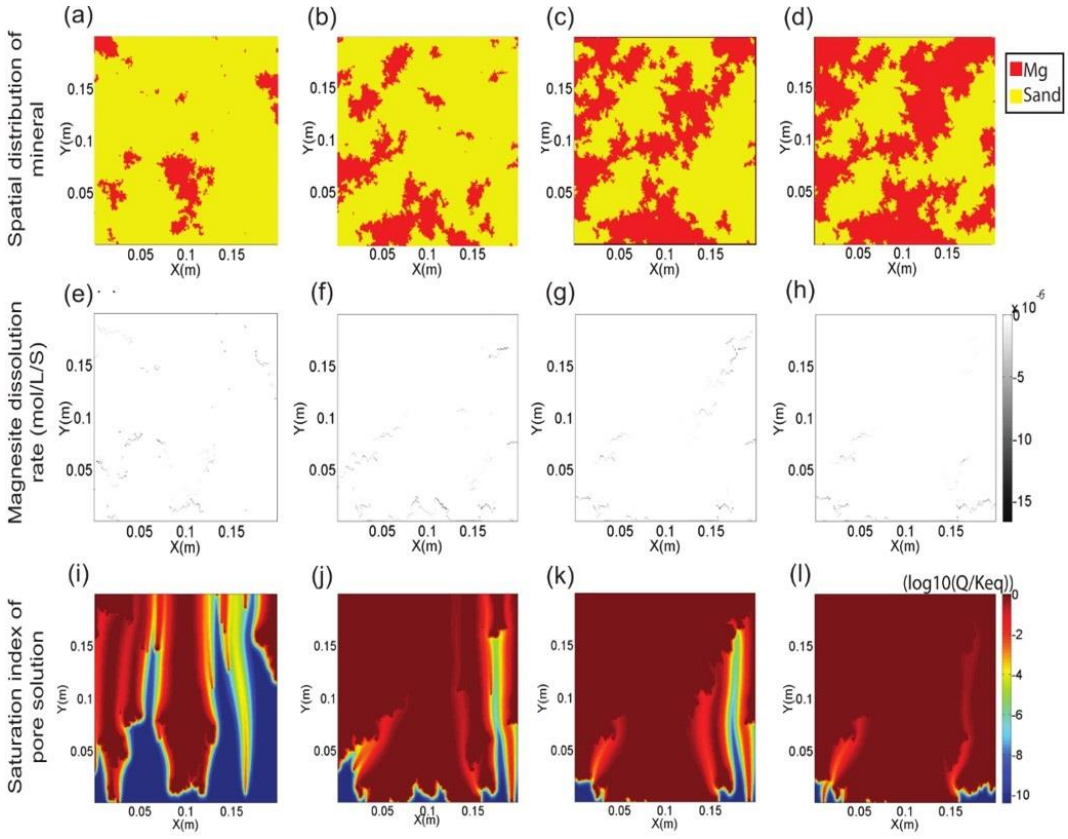

Figure 4.1 2D Spatial profiles of different percentage of magnesite: Images (a)–(d) show spatial distribution of mineral, (e)–(h) show magnesite dissolution rate, and (i)–(l) show saturation index of pore solution.

For Figure 4.2, shows the concentration of Mg2+ in different percentages of magnesite. As the percentage of magnesite increases, the concentration of Mg2+ also increases, and it has a significant change from 10% to 20% and at 40%, but just a slight change from 40% to 50%.

The same situation holds true in Figure4.3 where the pH value increases exponentially with different percentage increases of magnesite.

From Figure4.4, the average porosity increased with the percentage of magnesite increase, but the change was not significant. In Figure 4.5, the overall pore volume rate increased with the percentage of magnesite increase.

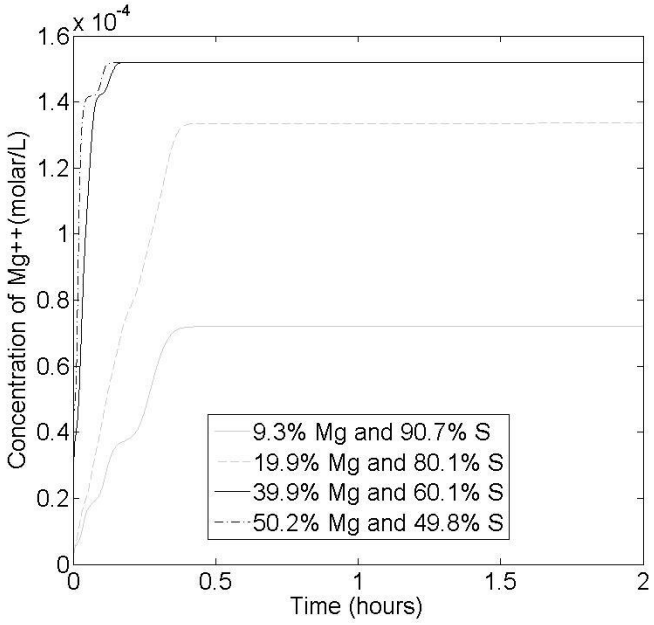

Figure 4.2 Concentration of Mg++ in different percentages of magnesite

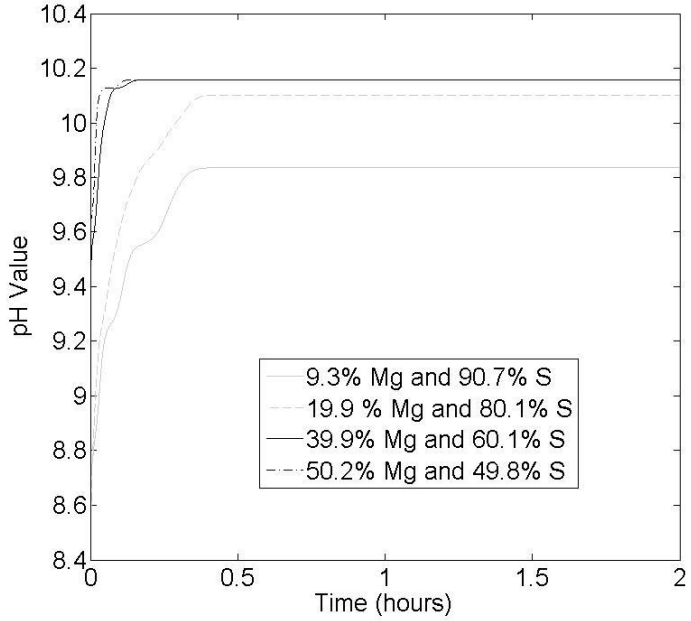

Figure 4.3 pH value according to different percentages of magnesite

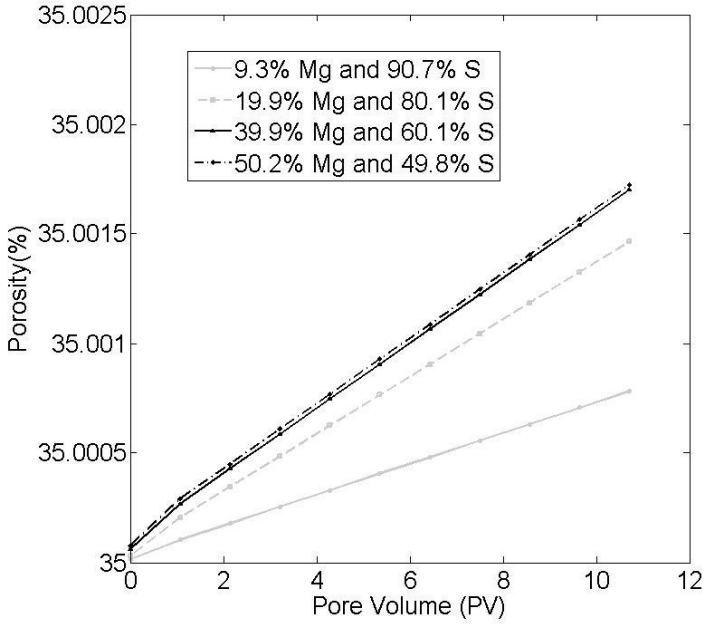

Figure 4.4 Average porosity in different percentages of magnesite

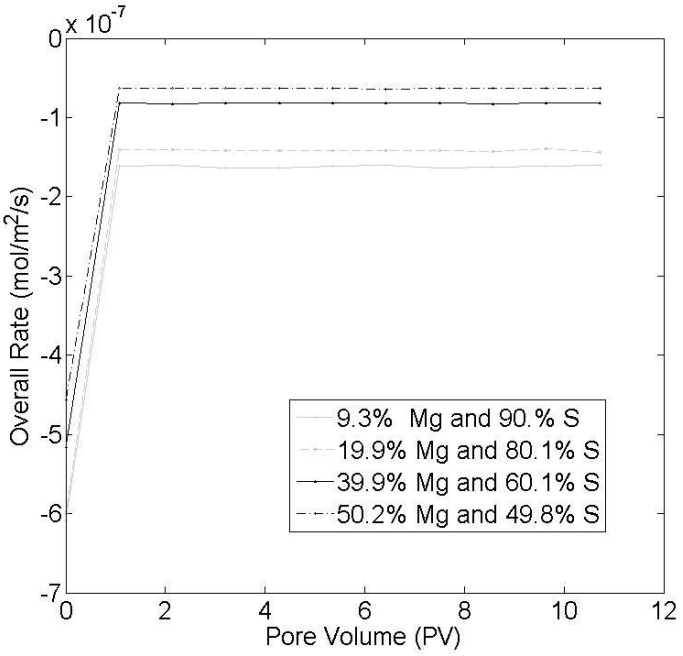

Figure 4.5 Overall rate in different percentages of magnesite

4.1.2. Permeability. The permeability of magnesite is a significant parameter of dissolution rate. With magnesite percentage increasing the dissolution rate also is decreasing.

The following represents three cases set apart for analysis according to different permeability levels of magnesite affecting the magnesite dissolution results. Table 4.2 illustrates the basic condition of three cases. The tested elements were magnesite and sand.

Figure 4.6 (a)–(c) shows the three cases' spatial distribution of magnesite and sand, as the same. Figures 4.6 (d)–(f) show the magnesite dissolution rate where the black part of the measuring column recorded the highest reaction rates.

The three figures are almost same in that the permeability did not change a lot of the magnesite dissolution rate.

Figure 4.6 (g)–(i) show the saturation index of pore solution, where higher permeability of magnesite put the readings into a redder zone, indicating a closeness to equilibrium conditions. So the higher the permeability of magnesite, closer the results are to equilibrium.

Figure 4.7, shows the concentration of Mg2+ in different permeability of magnesite and sand. With increases in the permeability of magnesite comes an increase in the concentration of Mg2+.

.

Table 4.2 Parameter of different permeability for three cases

	Flow rate	Sand permeability	Magnesite permeability	Major Anisotropy	Minor Anisotropy	Magnesite Percentage Initial	Sand Percentage Initial
a	5	1.00E-12	1.00E-13	50	50	0.093475	0.906525
b	5	1.00E-13	1.00E-13	50	50	0.093475	0.906525
c	5	1.00E-13	1.00E-12	50	50	0.093475	0.906525

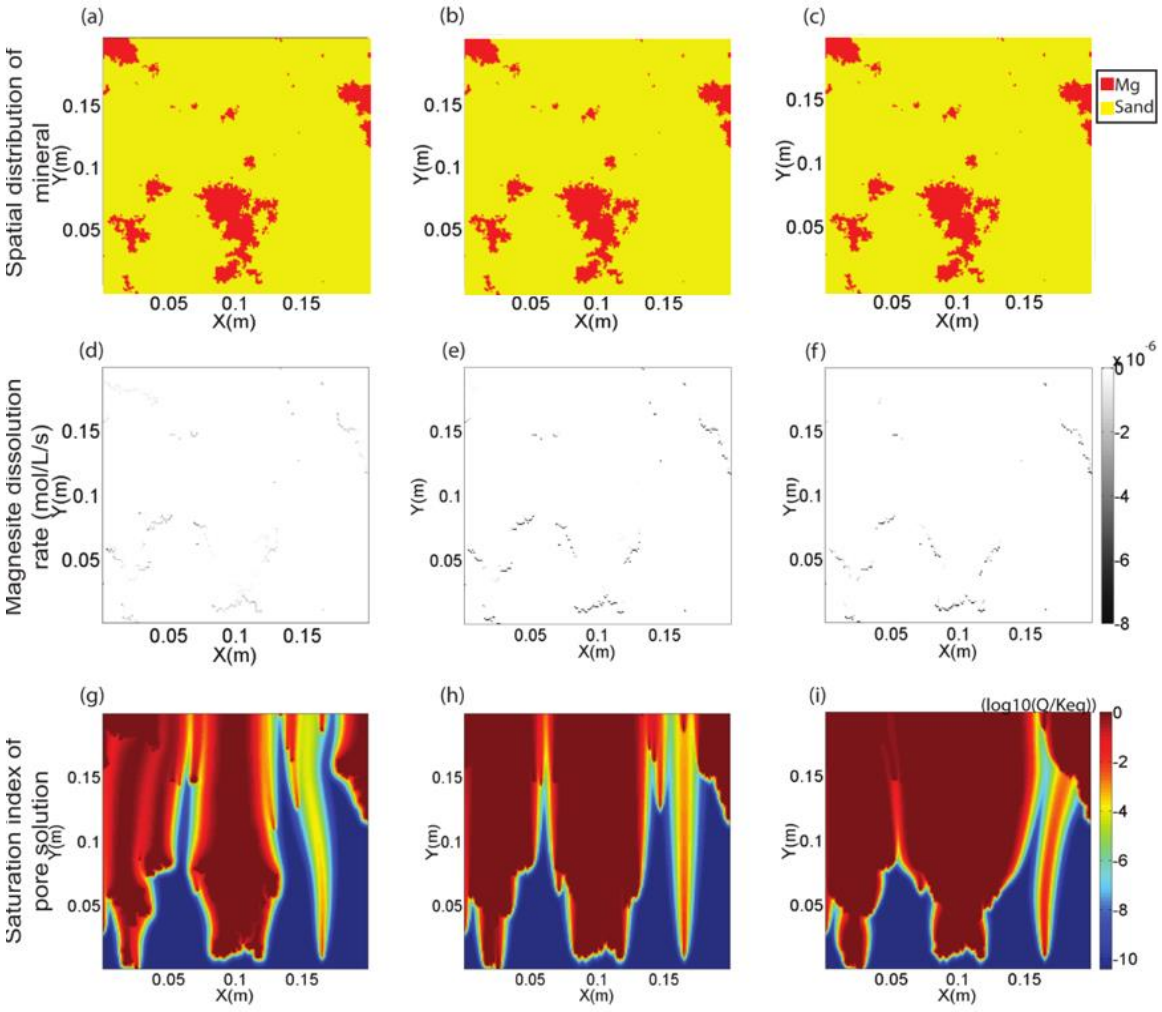

Figure 4.6 2D spatial profiles of different permeability of magnesite: (a)–(c) represent the spatial distribution of minerals (Mg is shown as red and sand as yellow); (d)–(f) shows the magnesite dissolution rate; (g)–(i) shows saturation index of pore solution.

Figure 4.8 pH value repeats the same situation. From Figure 4.9, shows an average porosity increase with the permeability of magnesite increase. However, Figure 4.10. shows an overall rate increase with the percentage of magnesite decrease.

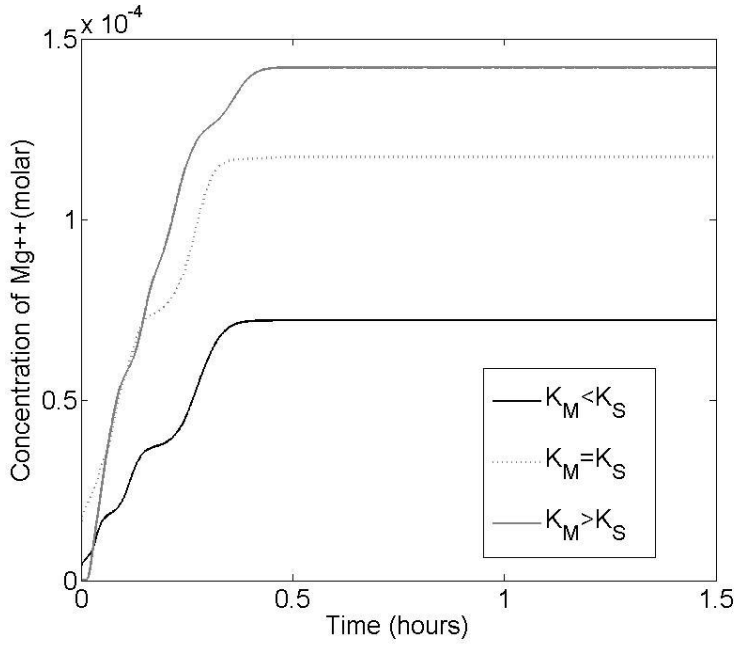

Figure. 4.7. Concentration of Mg++ at different permeability levels of magnesite

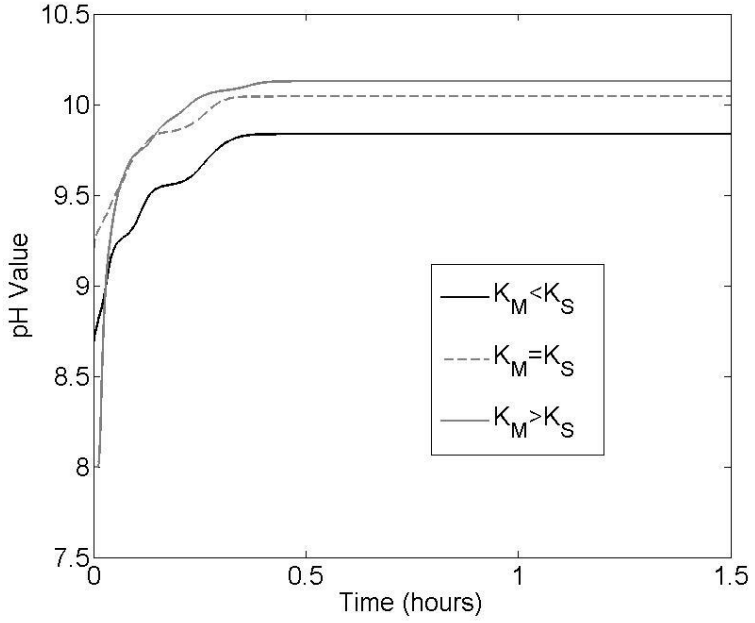

Figure. 4.8. pH value at different permeability levels of magnesite

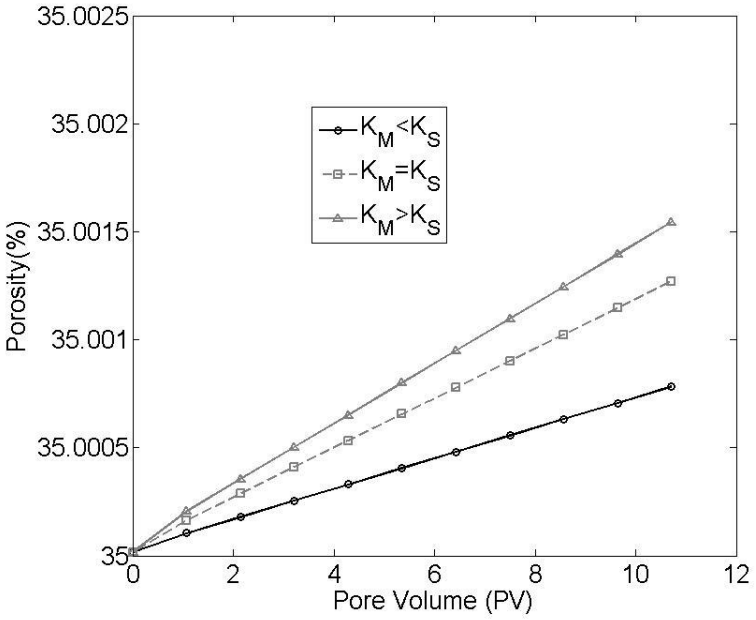

Figure. 4.9. Average porosity at different permeability levels

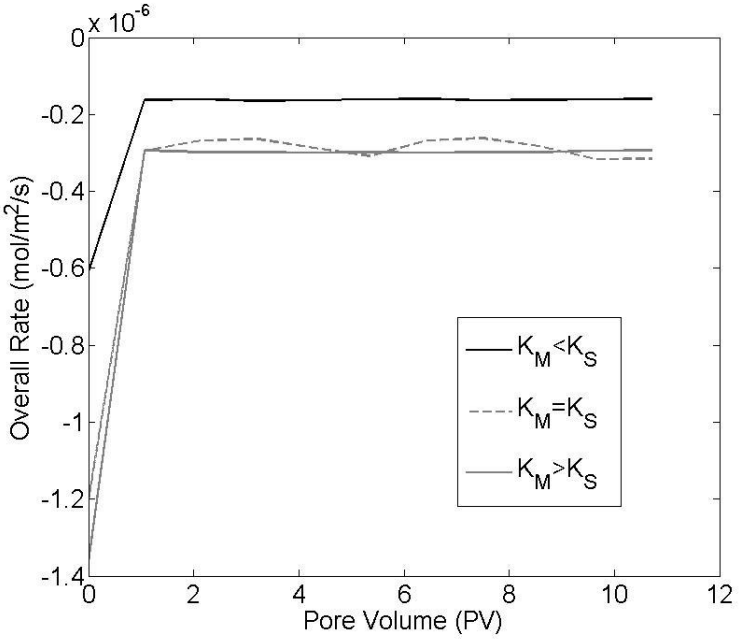

Figure 4.10. Overall rate in different permeability

4.1.3. Major Anisotropy. The major anisotropy of magnesite is a basic parameter of dissolution rate. When magnesite percentage increase the dissolution rate is also increase.

The following represents four typical case loads of magnesite and sand, which were analyzed to assess the effect of major anisotropy of magnesite for magnesite dissolution. Table 4.3 illustrates the basic parameters of the four cases. Although permeability rates were similar, major anisotropy differences due to magnesite increase were noted in (b)–(d).

Figure 4.11 (a)–(d) shows the four cases the spatial distribution of magnesite and sand. Figure 4.11 (e)– (h) show the magnesite dissolution rate with black color in the column showing high reaction rate. So a higher major anisotropy of magnesite can be assumed because magnesite has a high reaction rate. Figure 4.11(i)–(l) shows the saturation index of pore solution if the value is equal to zero, which translates to an equilibrium condition. From left to right, the redder zone decreased. So the lower major anisotropy of magnesite had higher saturation, closer to equilibrium conditions.

Table 4.3. The parameter of different major anisotropy

	Flow rate	Sand permeability	Magnesite permeability	Major Anisotropy	Minor Anisotropy	Magnesite Percentage Initial	Sand Percentage Initial
a	5	1.00E-12	1.00E-13	1	1	0.099124	0.90875
b	5	1.00E-12	1.00E-13	20	1	0.100725	0.899275
c	5	1.00E-12	1.00E-13	50	1	0.10065	0.89935
d	5	1.00E-12	1.00E-13	100	1	0.10195	0.89805

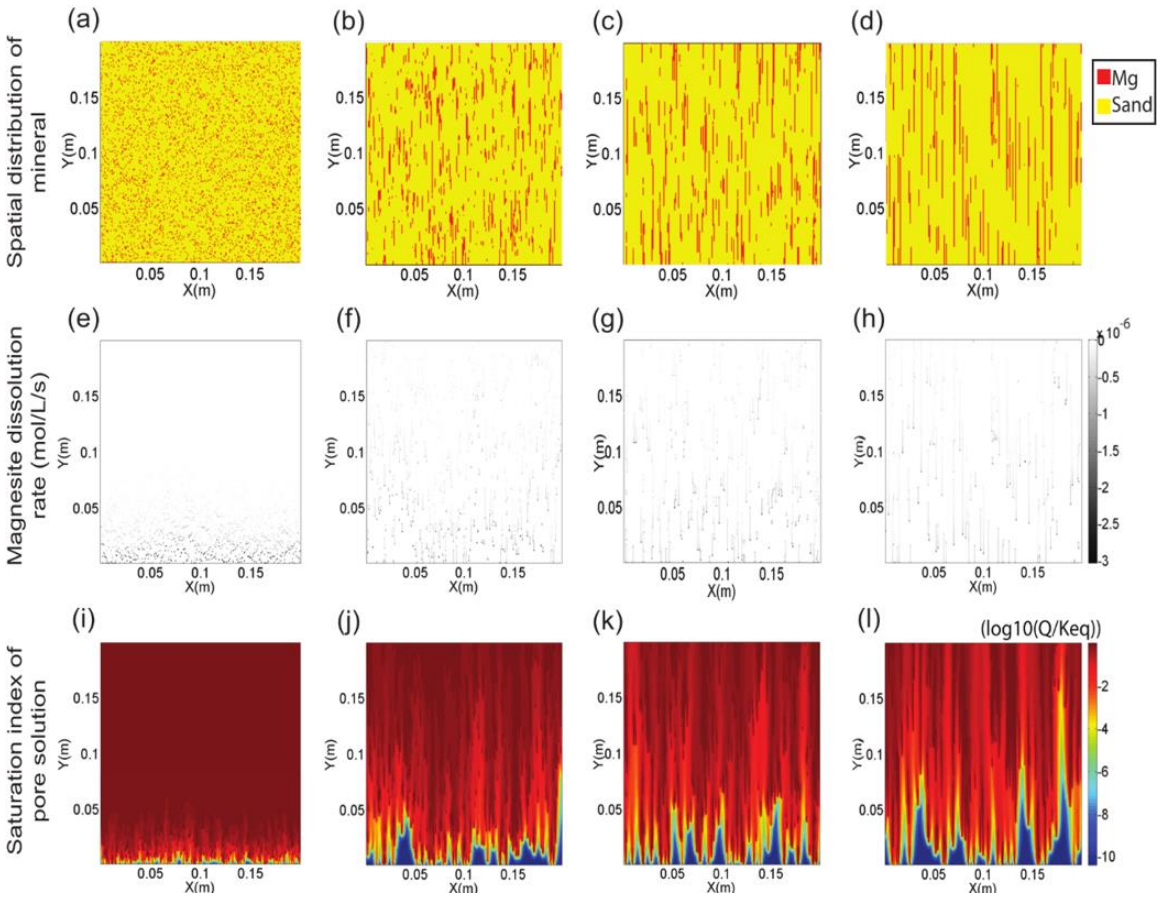

Figure 4.11 (a)–(d) shows 2D spatial proportions of magnesite and sand; (e)–(h) shows the magnesite dissolution rate; (i)–(l) represents saturation indices of pore solution.

For Figure 4.12, shows the concentration of Mg2+ in different major anisotropy reactions due to presence or quantity of magnesite. With the major anisotropy of magnesite increase the concentration of Mg2+ also decreasing. And for Figure 4.13 pH value also decreased when the major anisotropy increased.

In Figure 4.14 the average porosity increased with the major anisotropy of magnesite decreasing. On the contrary, in Figure 4.15. The overall rate increased with the major anisotropy of magnesite increasing.

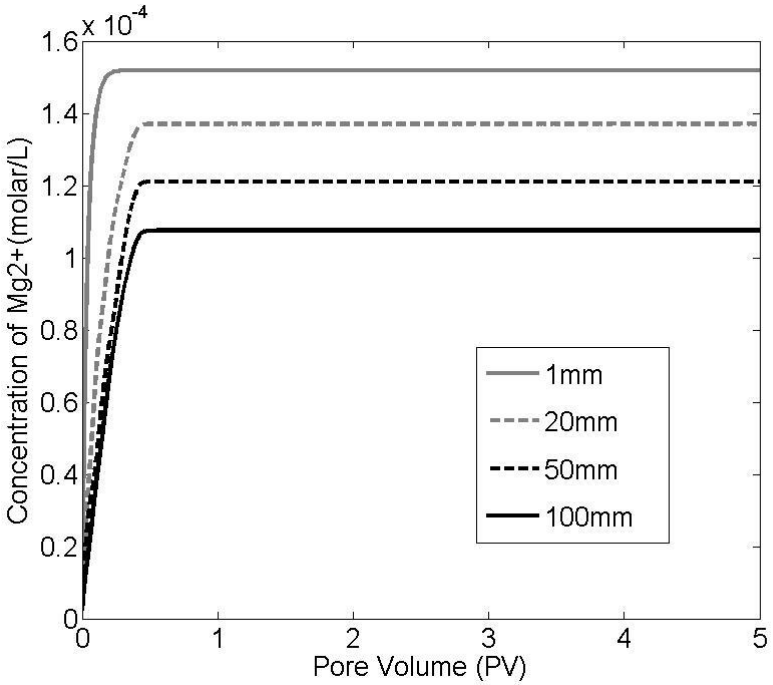

Figure 4.12. Concentration of Mg2+ in different major anisotropy

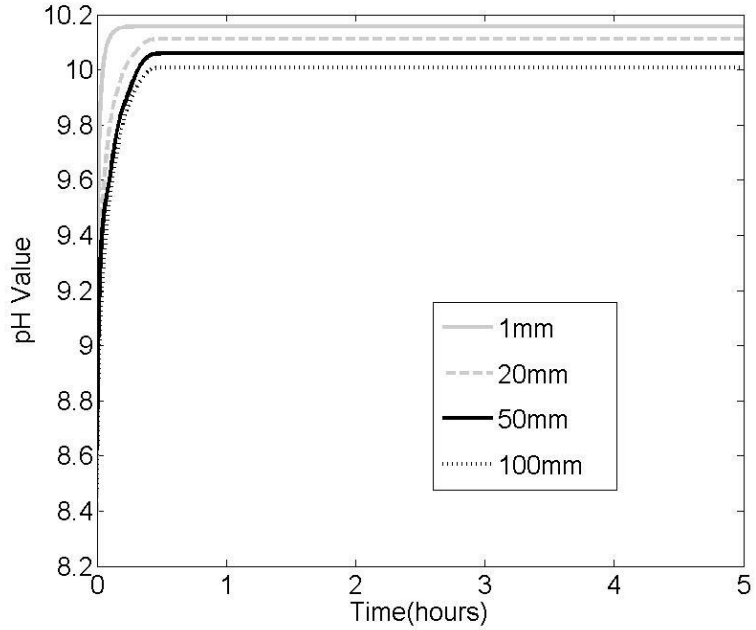

Figure 4.13. pH value in different major anisotropy

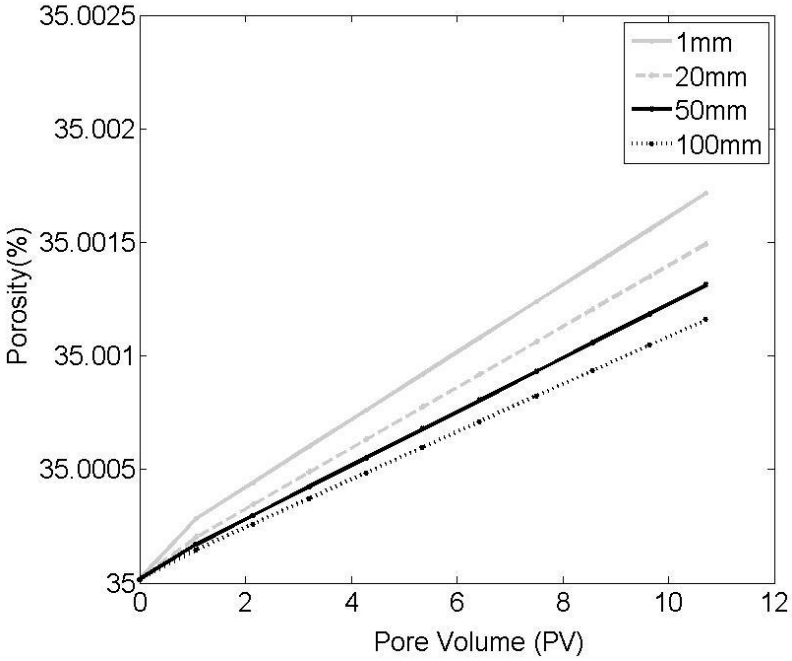

Figure 4.14. Average porosity in different major anisotropy

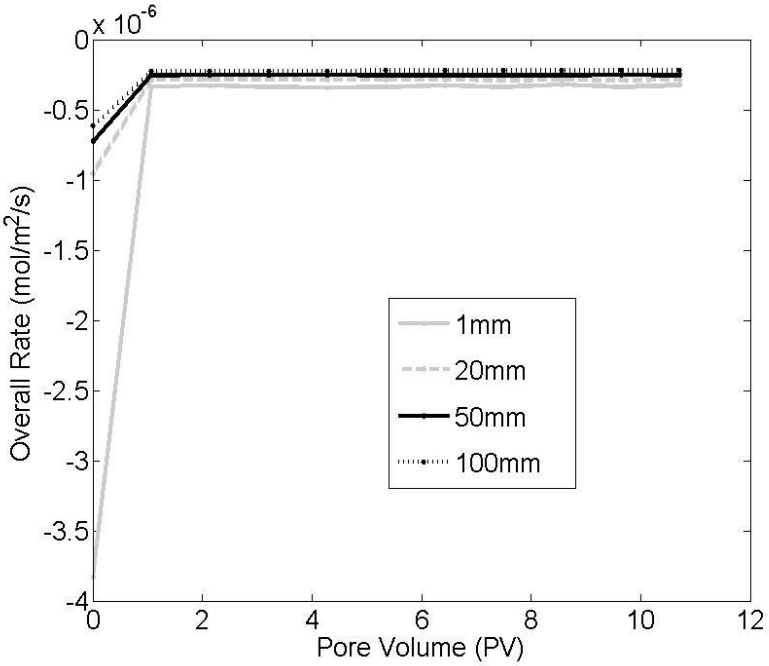

Figure 4.15. Overall rate in different major anisotropy

4.1.4. Minor Anisotropy. The minor anisotropy of magnesite is the last parameter of the basic parameter for dissolution rate. With magnesite, minor anisotropy increase as the dissolution rate decreases in most situations.

The following shows four caseloads of sand and magnesite analyzed to determine the effect of different minor anisotropy of magnesite for magnesite dissolutions. Table 4.4 illustrates the basic parameters of the contents of the four cases, with similar parameters comparable to the other figures with the same content at different sand/magnesite ratios, but with different minor anisotropy of magnesite.

And Figure 4.16 (a)–(d) shows the four cases with their spatial distribution of magnesite and sand, as from left to right, the minor anisotropy of magnesite increases. Figure 4.16 (e)– (h) shows the magnesite dissolution rate, as noted from left to right. It easy to see that lower major anisotropy of magnesite has a higher reaction rate.

Table 4.4. The parameter of different minor anisotropy

	Flow rate	Sand permeability	Magnesite permeability	Major Anisotropy	Minor Anisotropy	Magnesite Percentage Initial	Sand Percentage Initial
a	5	1.00E-12	1.00E-13	100	1	0.10195	0.89805
b	5	1.00E-12	1.00E-13	100	20	0.101025	0.898975
c	5	1.00E-12	1.00E-13	100	50	0.10205	0.89795
d	5	1.00E-12	1.00E-13	100	100	0.08935	0.91065

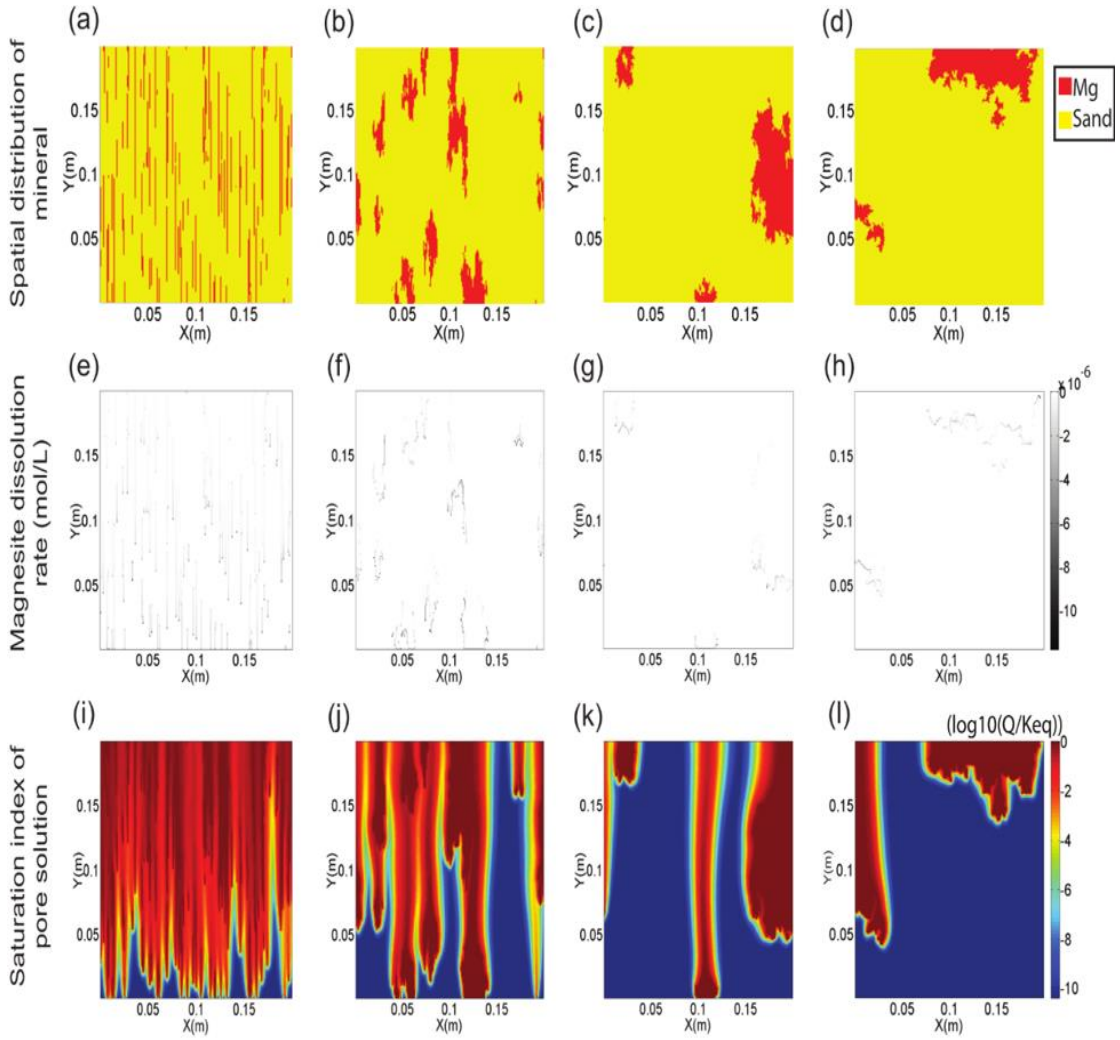

Figure 4.16 2D spatial profiles of different minor anisotropy of magnesite: (a)-(d) show spatial distribution of mineral;(e)-(h) show magnesite dissolution rate, and (i)-(l) represent saturation indices of pore solution.

Figure 4.16 (i)–(l) shows the saturation index of the pore solution. If the value is equal to zero, it indicates an equilibrium condition. From left to right, the redder zone decreases. So the lower minor anisotropy of magnesite has a higher saturation, and is closer to equilibrium conditions.

For Figure 4.17, shows the concentration of Mg2+ in different minor anisotropy of magnesite. When the minor anisotropy of magnesite increases, the concentration of Mg2+ also increases, but the100 mm of minor anisotropy of magnesite dissolution is higher than 50 mm.

This may be because the percentage of magnesite of 100 mm and 50 mm minor anisotropy was a little different. The same situation holds true for Figure 4.18 pH value and Figure 4.19 when looking at the average porosity.

However, what's different from the others is the Figure 4.20. overall rate increases with the minor anisotropy of magnesite decrease.

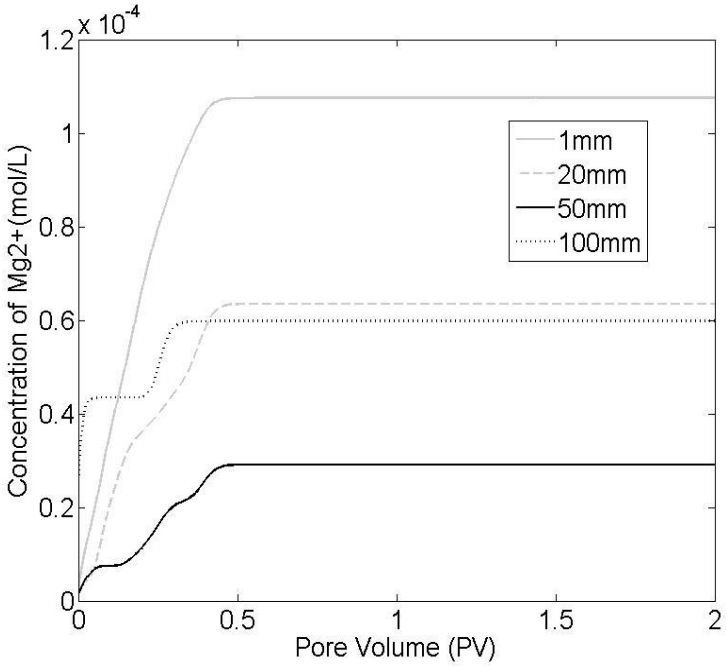

Figure 4.17. Concentration of Mg2+ in different minor anisotropy

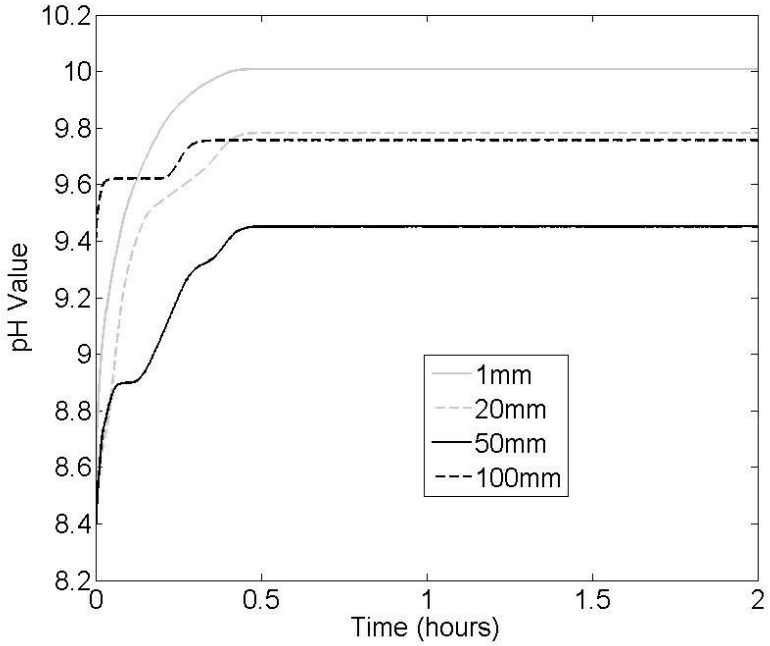

Figure 4.18. pH Value in different minor anisotropy

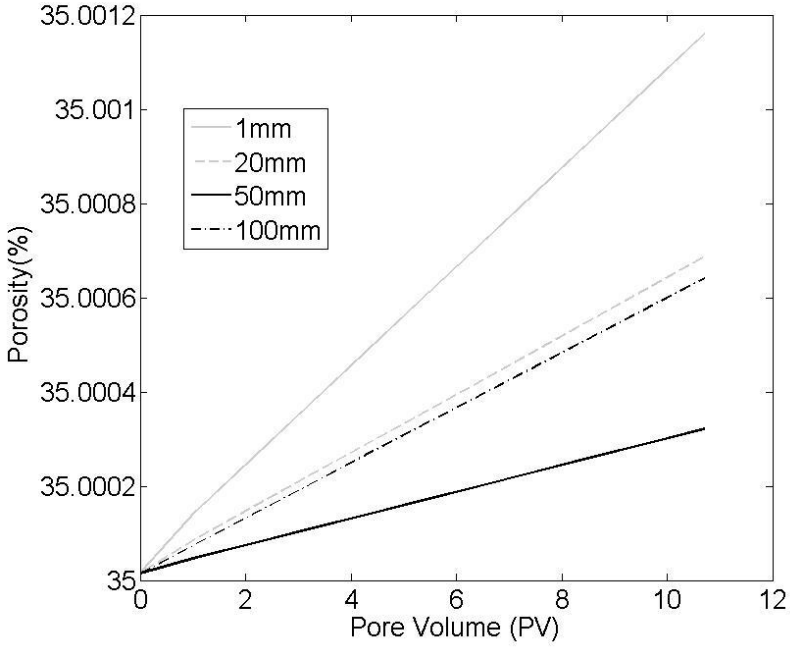

Figure 4.19. Average porosity in different minor anisotropy

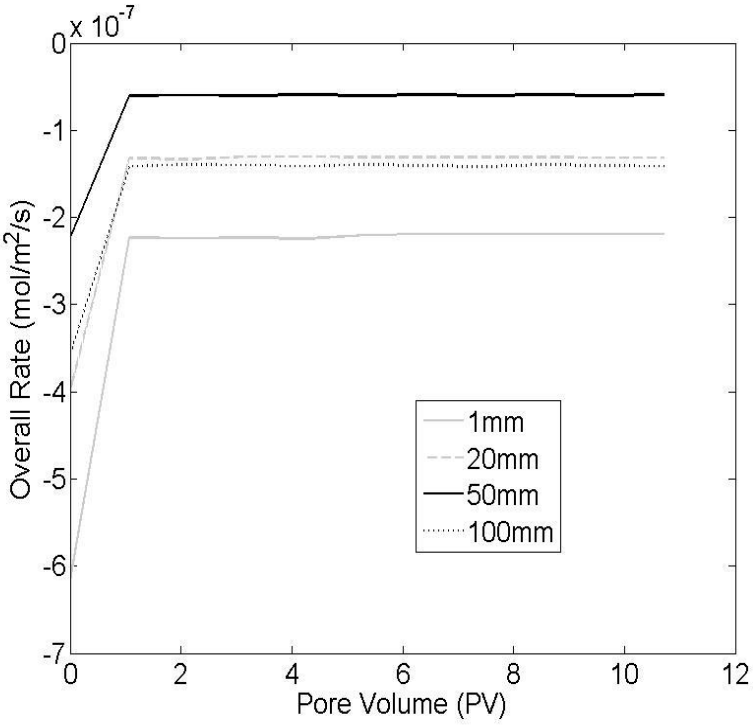

Figure 4.20. Overall rate in different minor anisotropy

4.2. BASIC PARAMETER REGRESSION ANALYSIS

After getting the results of the simulation, the next task was to analyze the data variance. The regression analysis is very meaningful. And get the results of regression analysis, can get more information such as the correlation coefficient, the trend of independent variance, and the dependent variances changing amplitude.

So, the regression analysis is a great method for this purpose, so a regression analysis of four basic parameters was used as independent variables and the overall rate and average porosity was used as dependent variables.

4.2.1. Percentage Regression Analysis. For the regression analysis of the different percentages of magnesite, Figure 4.21. and Figure 4.22. are under the same conditions as above results of percentage.

From Figure 4.21., the overall rate increase with the percentage of magnesite increased and Figure 4.22 the average porosity remained in the same situation. So under the other conditions are same, only the percentage of magnesite different situation, the percentage of magnesite had a positive correlation with porosity and magnesite and for the overall rate gained a strong correlation.

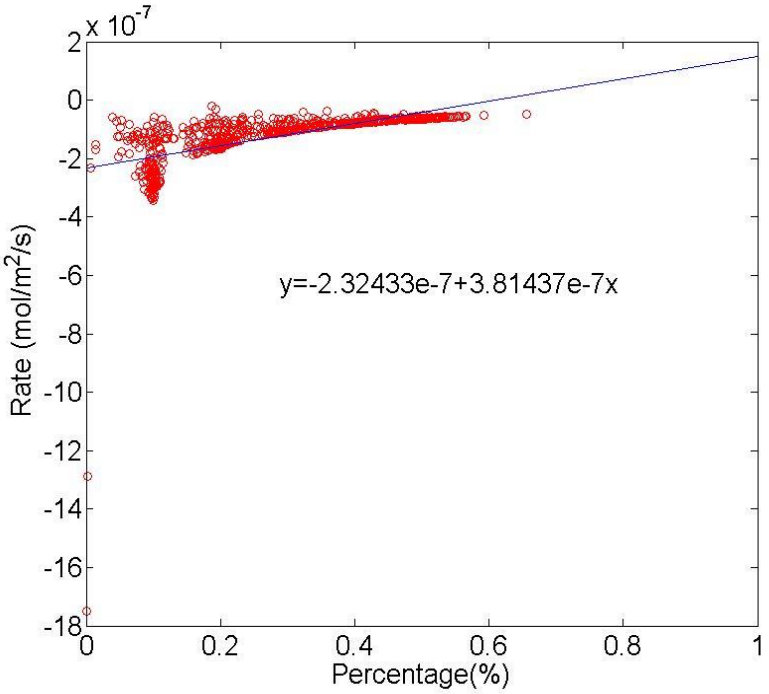

Figure 4.21 Rate plot of regression analysis of partial data of different percentage of magnesite

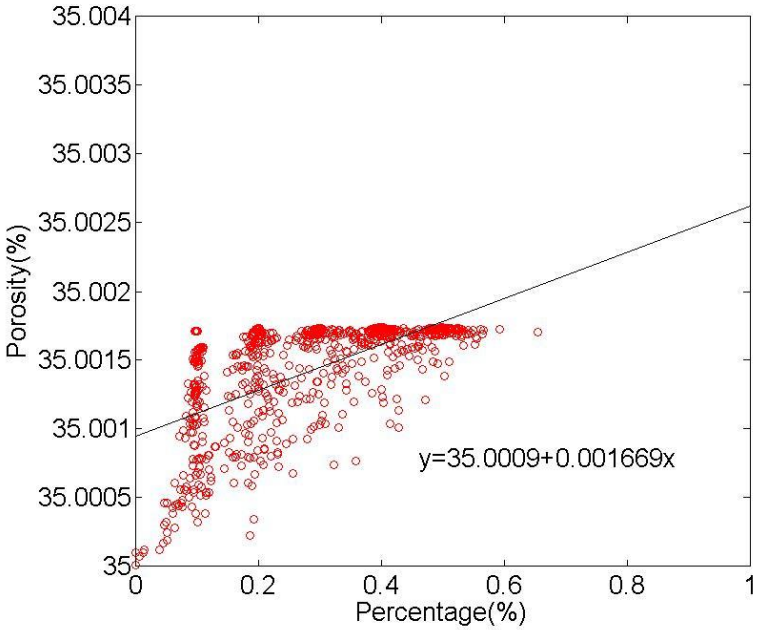

Figure 4.22. Porosity plot of regression analysis of partial data of different percentages of magnesite.

The following Figure 4.23 and Figure 4.24 are used for all of the data of the thesis, Figure 4.23. shows the data points are an almost closed line of the equation. So the percentage is a very important element of the overall rate. And it means the percentage of magnesite has a very strong relationship with the overall rate.

In Figure 4.24, the partial percentages of data are really close to the line of the equation, but some of the data are far away from that line. Hence, the figure illustrates how other parameters can have an important effect on the average of porosity. But compare the Figure 4.23 and Figure 4.24, easy to know the percentage of magnesite with overall rate correlation coefficient bigger than the percentage of magnesite with the average porosity of correlation coefficient.

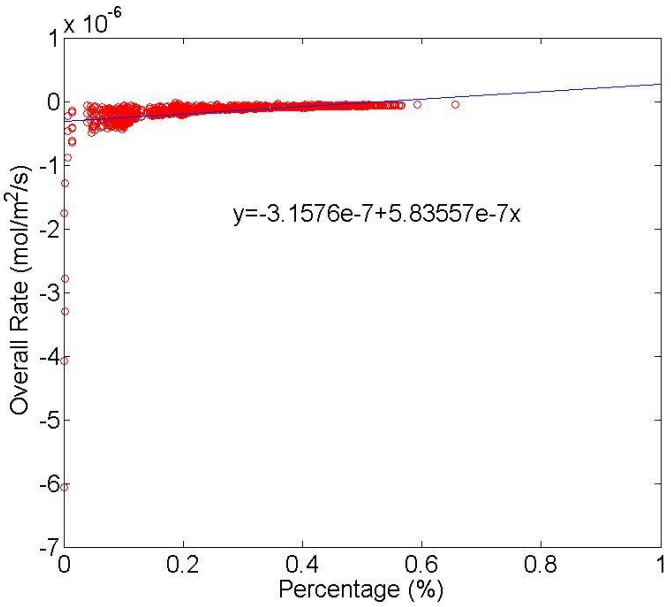

Figure 4.23. Regression analysis of total data of relationship between different percentages of magnesite and overall rate

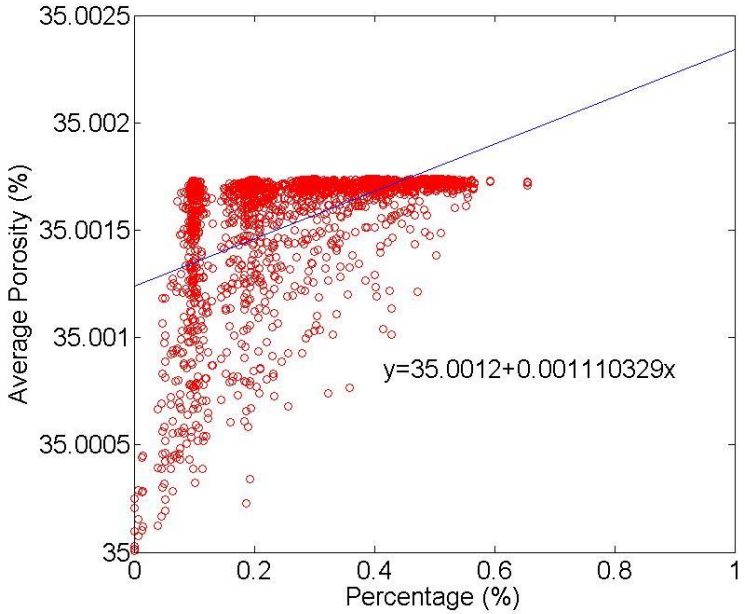

Figure 4.24. Regression analysis of total data of relationship between different percentages of magnesite and average porosity

4.2.2. Permeability Regression Analysis. The permeability is listed in Table 4.5. From Figure 4.25. and Figure 4.26, the overall rate has a positive correlation with the permeability of sand.

Table 4.5. Permeability for all cases

	Sand Permeability (m^2)	Magnesite Permeability (m^2)
a	1.00E-12	1.00E-13
b	1.00E-13	1.00E-13
c	1.00E-13	1.00E-12

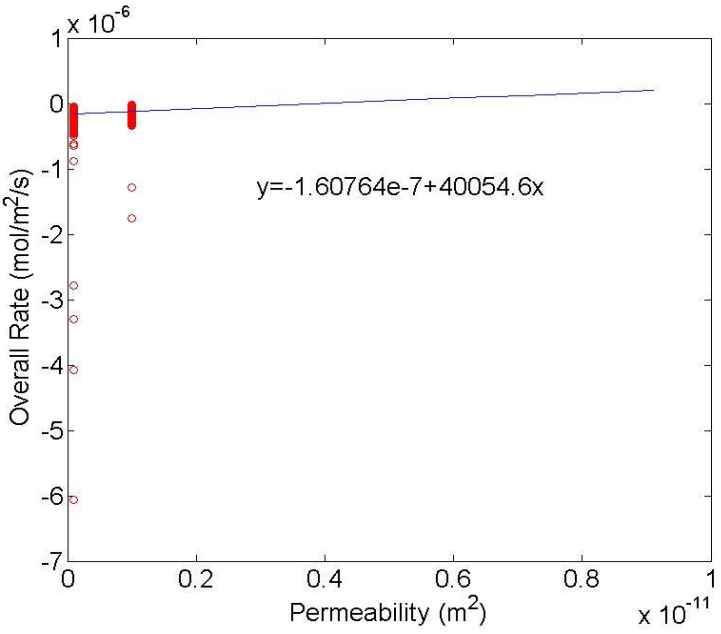

Figure 4.25. Regression analysis of total data of the relationship between the different permeability levels of sand and overall rates.

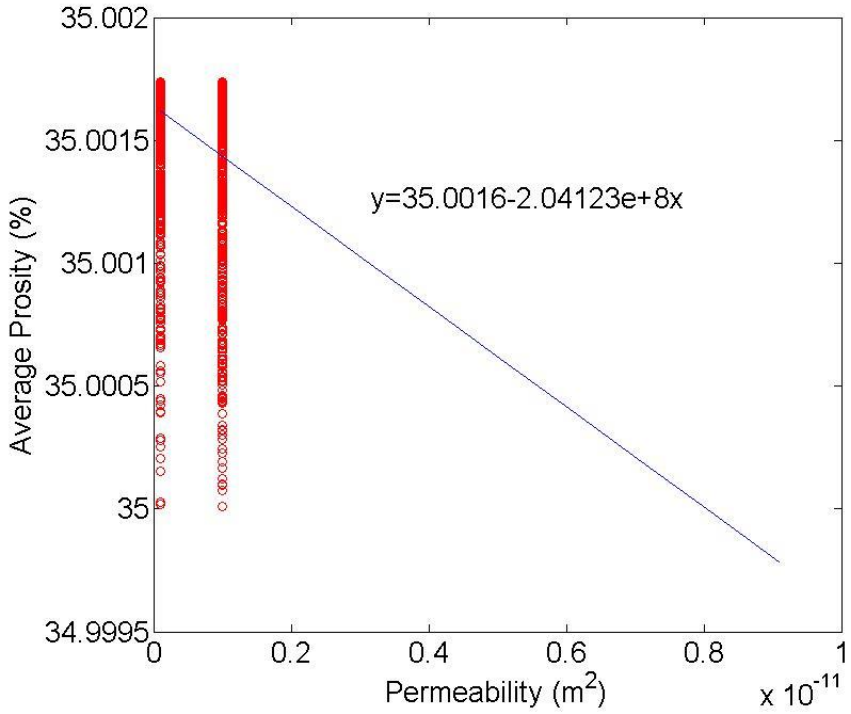

Figure 4.26. Regression analysis of total data of the relationship between the different permeability levels of sand and average porosity.

But Figure 4.25. and Figure 4.26 the average has a negative correlation with the permeability of sand, because the data points are away from the line of the equation. So the permeability of sand has a weak correlation with overall rates and average porosity.

For permeability of magnesite, don't have a correlation with overall rate because the value of P is 0.5490, which means it is above 0.005.

However, the permeability of magnesite has a correlation with average porosity, even though it is a weak positive correlation.

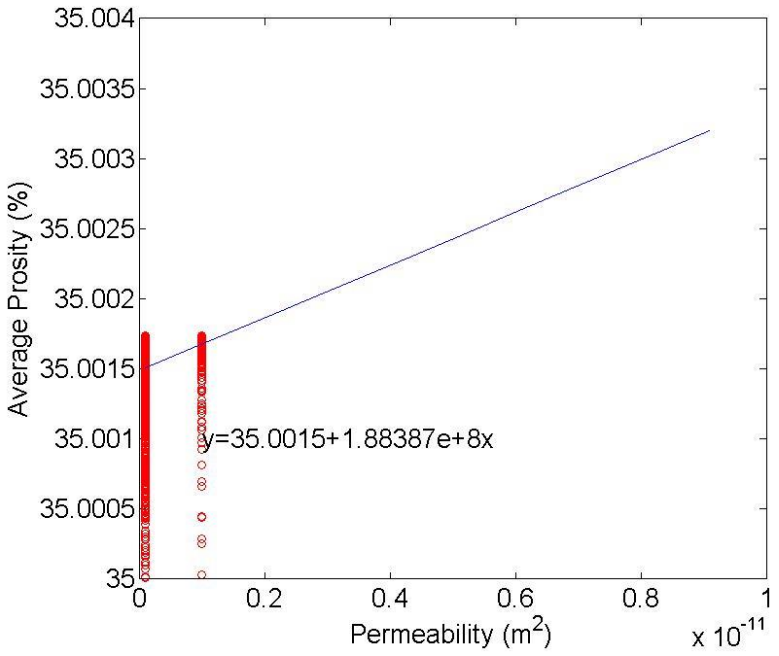

Figure 4.27. Regression analysis of total data of the relationship between the different permeability of magnesite and average porosity.

4.2.3. Major Anisotropy Regression Analysis. For Figure 4.28 and Figure 4.29 in regression analysis have the same permeability of magnesite and sand which is different in major anisotropy of magnesite.

And from the two Figures, easy to know that whatever the overall rate or average porosity, there is a very weak correlation with major anisotropy. For overall rate has a positive correlation, while average porosity has a negative correlation.

For all data herein, the major anisotropy of magnesite does not have a correlation with the overall rate because the value of P is 0.0311> 0.005, so the major anisotropy of magnesite cannot affect the overall rate. However, the major anisotropy of magnesite has a weak negative correlation with average porosity.

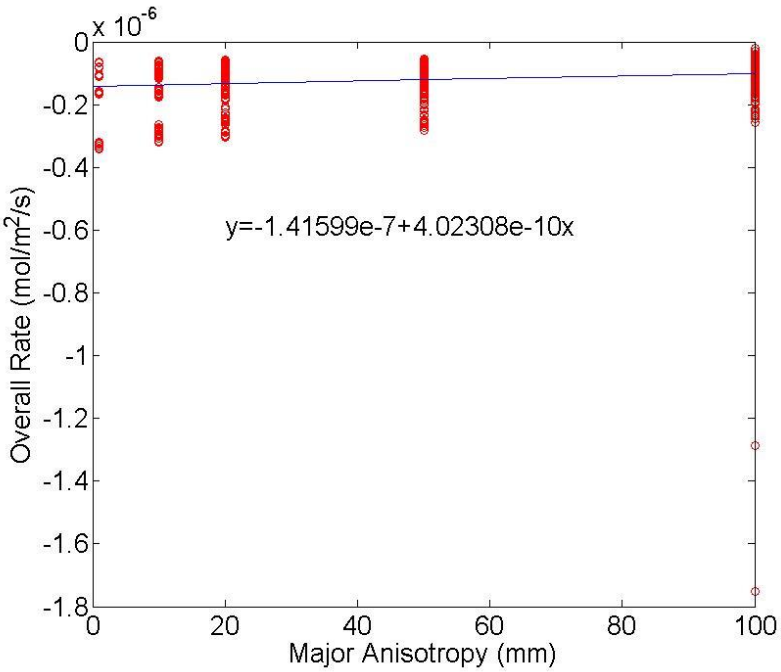

Figure 4.28. Regression analysis of partial data of relationship between different major anisotropy of magnesite and overall rate

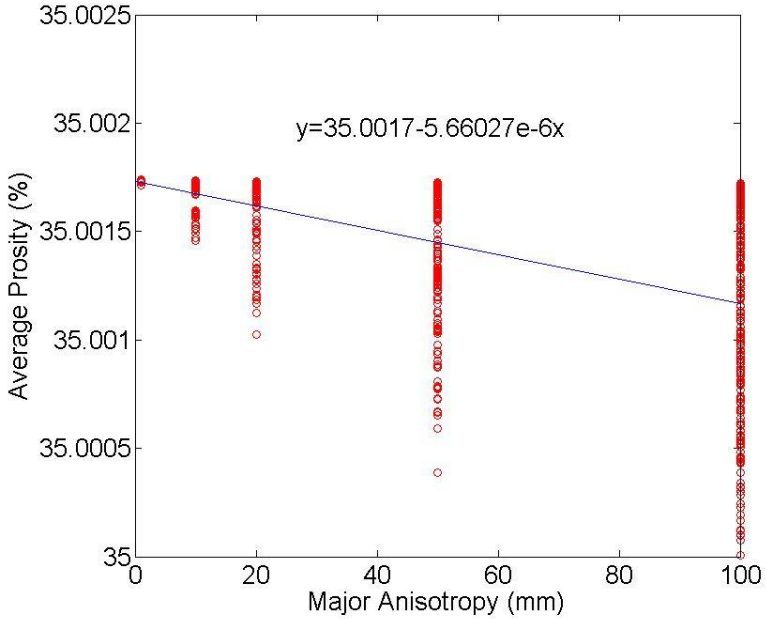

Figure 4.29 Regression analysis of partial data of relationship between different major anisotropy of magnesite and average porosity

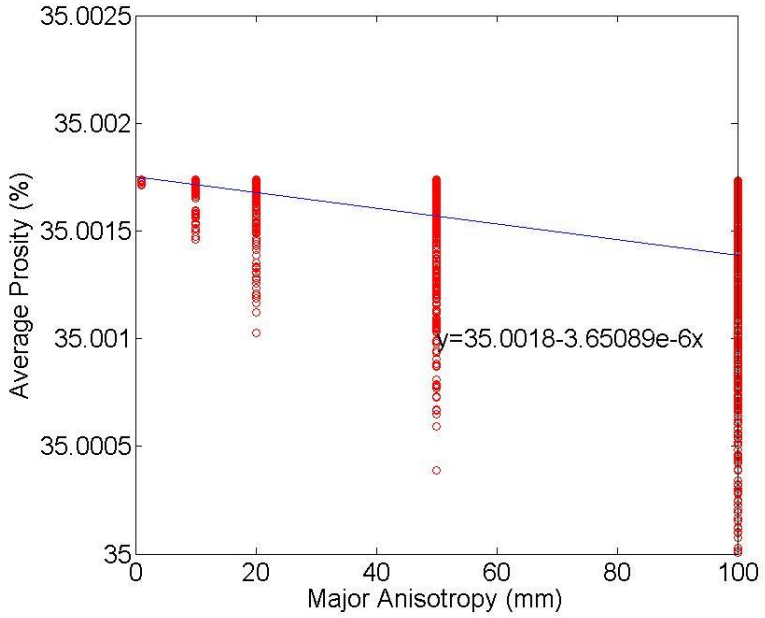

Figure 4.30. Regression analysis of total data of relationship between different major anisotropy of magnesite and average porosity

4.2.4. Minor Anisotropy Regression Analysis. For Figure 4.31 in regression analysis have the same permeability of magnesite and sand, and the permeability of sand is greater than the permeability of magnesite and different from the minor anisotropy of magnesite. For minor anisotropy of magnesite in this situation is non-correlation with the overall rate, because the P value is 0.4232>0.005. Nevertheless, for average porosity there is a very weak negative correlation with minor anisotropy.

Figure 4.32. and Figure 4.33 shows all data in the thesis and includes different minor anisotropy of magnesite. For two figures, both of them show most of the data points as being away from the line of the correlation equation. As a result, the correlation is very weak. Whatever average porosity or overall rate, they both have a negative correlation with minor anisotropy of magnesite.

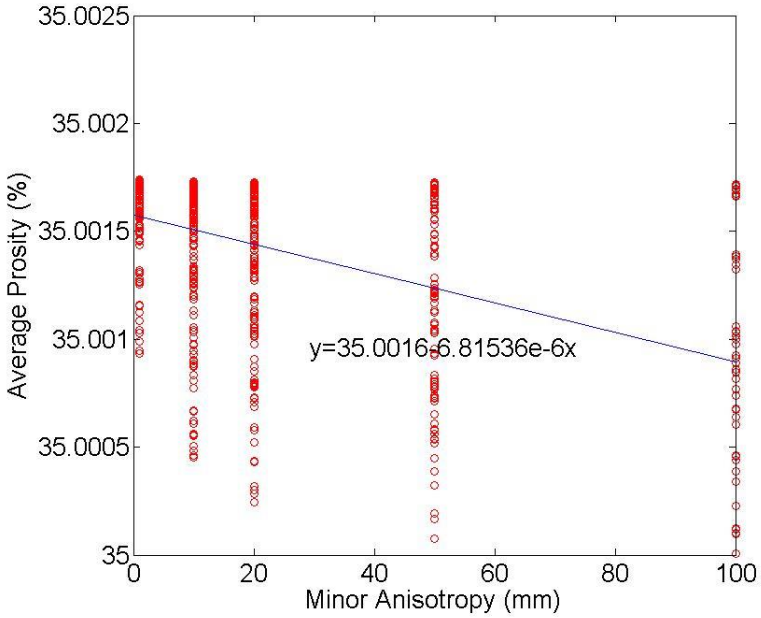

Figure 4.31. Regression analysis of partial data of relationship between different minor anisotropy of magnesite and average porosity

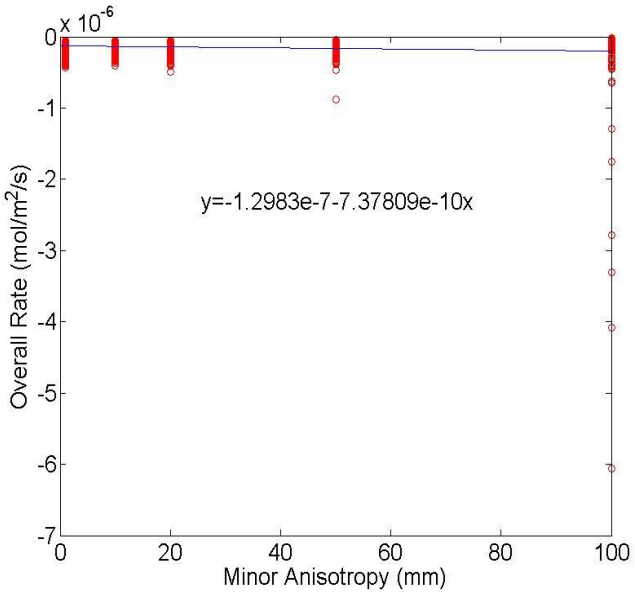

Figure 4.32. Regression analysis of total data of relationship between different minor anisotropy of magnesite and overall rate

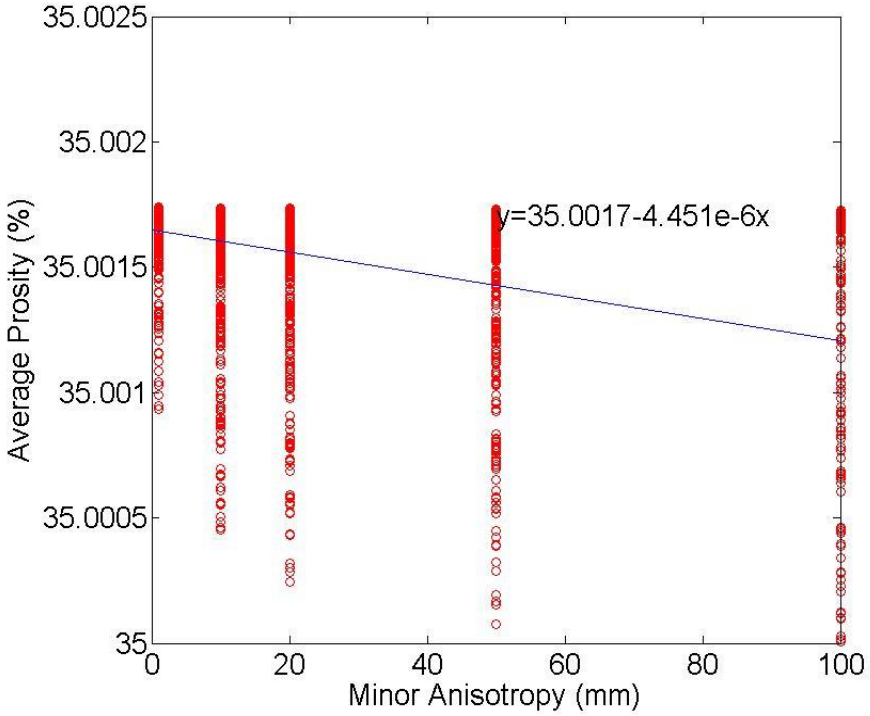

Figure 4.33. Regression analysis of total data of relationship between different minor anisotropy of magnesite and average porosity

4.2.5. Mean and Confidence. After regression analysis, here is the mean of percentage of magnesite and mean of average porosity and overall rate (red points). The mean for each group has all same conditions. One must also calculate the confidence (green points) of the regression analysis equation (blue line), Figure 4.34. and Figure 4.35 show the almost mean to be in the 95% confidence intervals. It means the confidence level is very high. The Figure 4.36 and Figure 4.37 show the relation between the major anisotropy and mean of average porosity as well as an overall rate (red points).

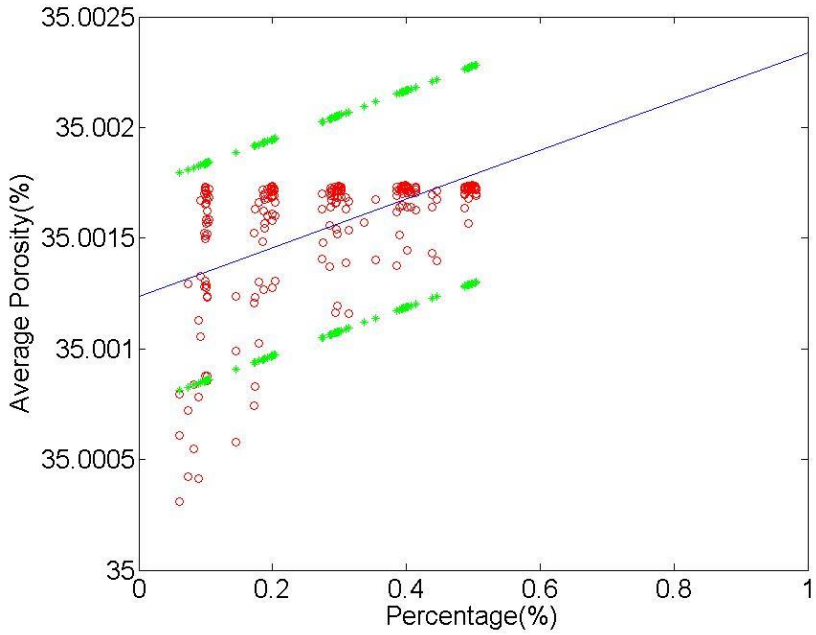

Figure 4.34. Mean and confidence of percentage and average porosity

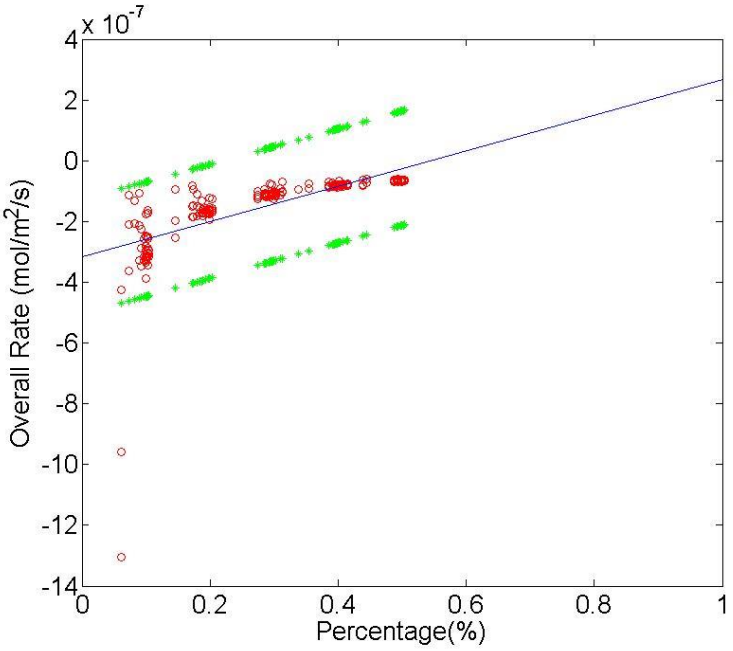

Figure 4.35. Mean and confidence of percentage and overall rate

The Figure 4.36 and Figure 4.37. each point representing the group has all the same conditions. We also calculated the confidence (green points) of the regression analysis equation (blue line) from Figure 4.36. and Figure 4.37. These figures illustrate how the mean points are in the confidence intervals, which means confidence level is very high level.

The Figure 4.38. and Figure 4.39 show the relation between the minor anisotropy and mean of average porosity and overall rate (red points). Each point represents the group that has all same conditions. Green points represent confidence.

The blue line stands for the regression analysis equation. Figure 4.38. is part of the mean and represents confidence intervals. Figure 4.39 has mean points that are almost in the confidence intervals, which means the confidence level rate is higher than the confidence level of porosity.

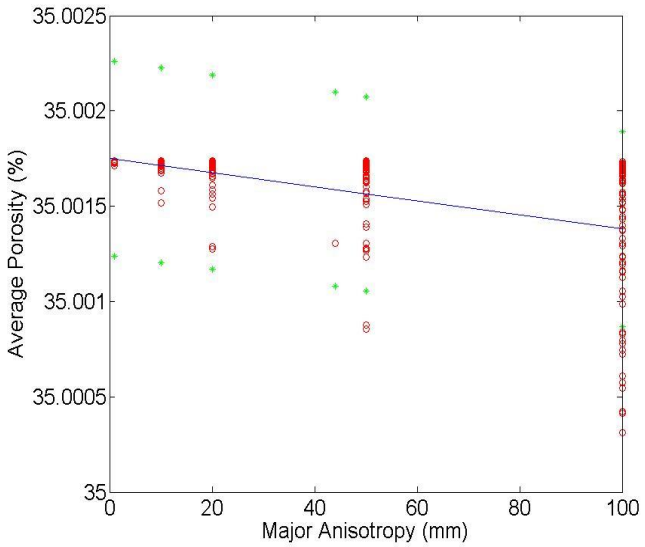

Figure 4.36. Mean and confidence of major anisotropy and average porosit

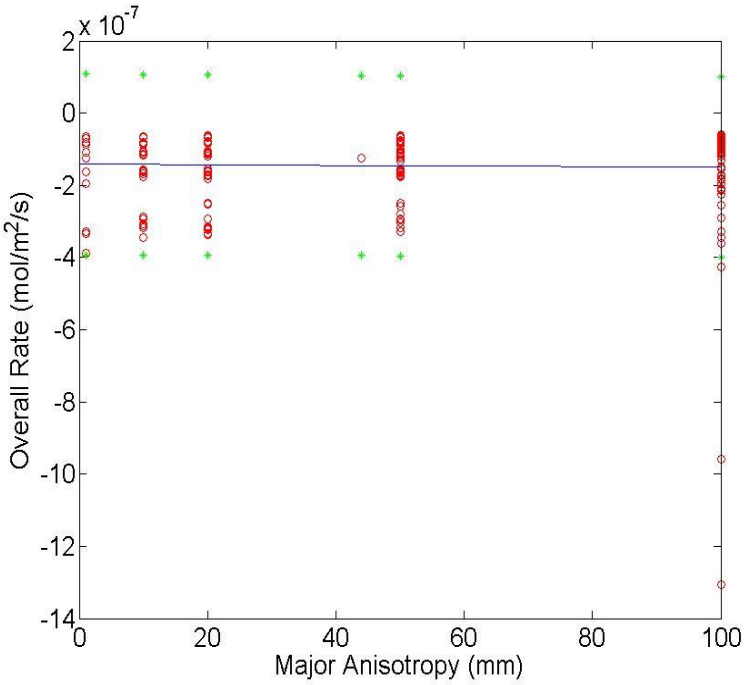

Figure 4.37. Mean and confidence of major anisotropy and overall rate

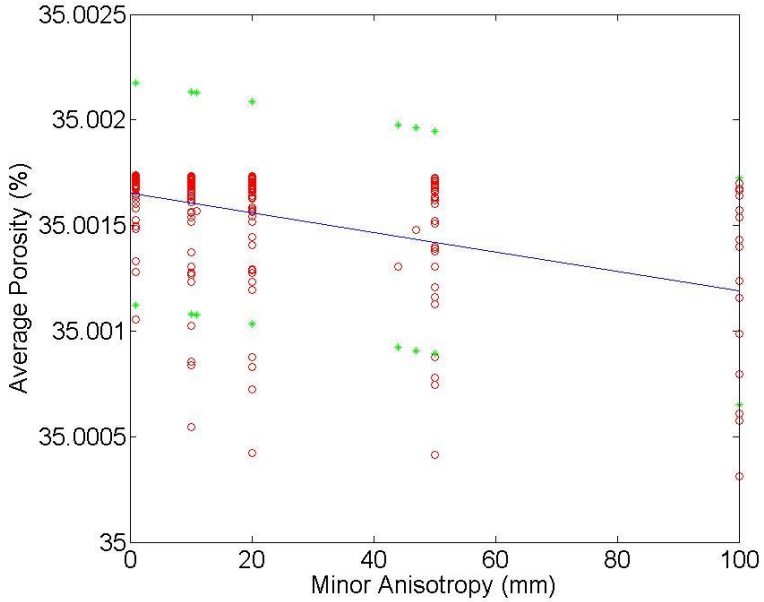

Figure 4.38. Mean and confidence of minor anisotropy and average porosity

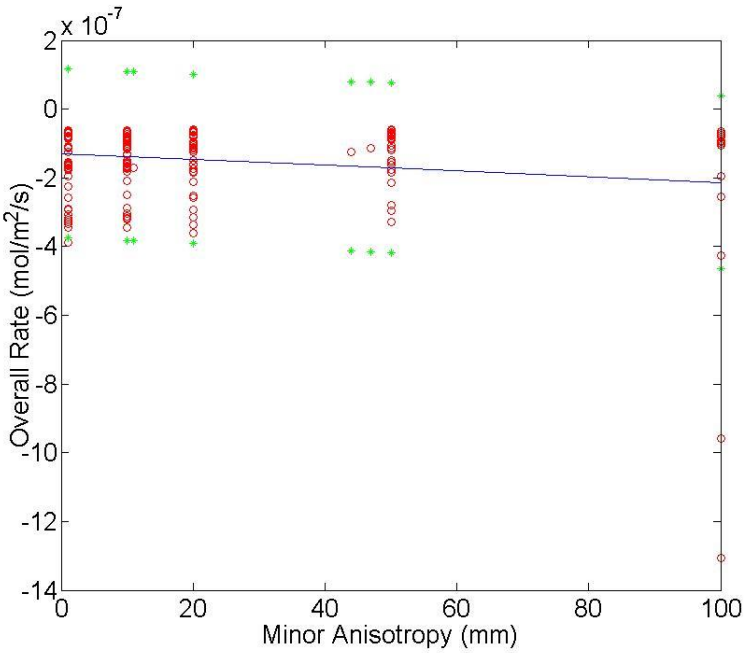

Figure 4.39. Mean and confidence of minor anisotropy and overall rate

4.3. ANALYSIS OF VARIANCE

Before analysis, single parameters are often discussed, but usually there are multiple variables involved. In the analysis that follows, several parameters are given for overall rates and average porosity.

Table 4.5. has three different permeability levels, so in this part we analysis each permeability level and then analysis total data. And get the summery of the

Because the permeability of magnesite is equal to the permeability of sand, we did a regression analysis for the independent variate of average porosity and overall rates. From Table 4.6 and the equation, for overall rate non-correlation with major anisotropy, stronger correlation came with an increase in the percentage of magnesite.

Average porosity also has a very strong correlation with percentage of magnesite. And, as can be expected, minor anisotropy has a negative correlation with rate and porosity, but the percentage of magnesite has a positive correlation with rate and porosity.

An overall rate correlation equation and average porosity equation follow:

$$R=-3.40286e\text{-}7-9.68562e\text{-}10x_2+6.23877e\text{-}7x_3 \quad (17)$$

$$\emptyset=35.0015-2.6511e\text{-}6x_1-1.83421e\text{-}6x_2+0.00100401x_3 \quad (18)$$

Table 4.6. Multivariate parameter for regression analysis of same permeability

	Overall Rate p-Val	Overall Rate t-stat	Average Porosity p-Val	Average Porosity t-stat
Major anisotropy(x_1)	0.0150>0.005	2.4384	0.0000	-13.2050
Minor anisotropy(x_2)	0.0003<0.005	-3.5961	0.0000	-6.4346
Percentage of magnesite(x_3)	0.0000	14.6855	0.0000	22.3303

In the next analysis 10 times of permeability of magnesite is equal to the permeability of sand. From Table 4.7 and equation, for overall rate non-correlation with minor anisotropy and correlation with major anisotropy is weakly negative; for percentage, rates are positive.

In average porosity, minor and major anisotropy is negative, but the correlation with percentage of magnesite is strongest and it is positive. For overall rate correlation, equation and average porosity equations follow:

$$R=-2.59143e-7-4.79779e-10x_1+3.87576e-7x_3 \quad (19)$$

$$\emptyset=35.0012-3.67371e-6x_1-3.67371e-6x_2+0.0019013x_3 \quad (20)$$

Table 4.7. Multivariate parameter for regression analysis of $10k_{mg} = k_{sand}$

	Overall Rate p-Val	Overall Rate t-stat	Average Porosity p-Val	Average Porosity t-stat
Major anisotropy(x_1)	0.0000	6.1507	0.0000	-17.3600
Minor anisotropy(x_2)	0.5300>0.005	-0.6282	0.0000	-10.8979
Percentage of magnesite(x_3)	0.0000	19.6373	0.0000	30.1116

At permeability of magnesite is equal to 10 times the permeability of sand regression analysis. Table 4.8 and equations (21) and (22) cover overall rate non-correlation with major anisotropy and positive correlation with percentage of magnesite and minor anisotropy.

And average porosity has a strong correlation as a percentage of magnesite. Then the minor and major anisotropy has a negative correlation with rate and porosity. Overall rate correlation and average porosity can be calculated as follows:

$$R=-3.47503e-7-1.3772e-10x_2+7.3347e-7x_3 \quad (21)$$

$$\emptyset=35.0016-1.0953e-6x_1-1.79105e-6x_2+0.000553429x_3 \quad (22)$$

Table 4.8. Multivariate parameter for regression analysis of $k_{mg} = 10k_{sand}$

	Overall Rate p-Val	Overall Rate t-stat	Average Porosity p-Val	Average Porosity t-stat
Major anisotropy(x_1)	0.5983>0.005	0.5270	0.0000	-6.23634
Minor anisotropy(x_2)	0.0000	-4.1447	0.0000	-7.2214
Percentage of magnesite(x_3)	0.0000	12.3880	0.0000	14.2099

Finally, the regression analysis is for all data is in the thesis. Table 4.9 and equation covers overall rate non-correlation with the sand permeability and stronger correlation with percentage of magnesite, and only has a negative correlation with minor anisotropy while others show a positive correlation. For average porosity, one must have a strong correlation with percentage of magnesite. The minor and major anisotropy and permeability of magnesite have a negative correlation with rate and porosity. The percentage of magnesite and permeability of sand has a positive correlation with them. Overall rate correlation equation and average porosity can be written as:

$$R=-3.33468e-7+40065x_1+3.70077e-10x_3-8.42368e-10x_4+5.81934e-7x_5 \quad (23)$$

$$\emptyset=35.0015-1.52212e+8x_1+1.05799e+8x_2-2.60096e-6x_3-2.44968e-6x_4+0.00104478x_5 \quad (24)$$

Table 4.9. Multivariate parameter for regression analysis of total data

	Overall Rate p-Val	Overall Rate t-stat	Average Porosity p-Val	Average Porosity t-stat
Magnesite permeability(x_1)	0.0000	40065	0.0000	-13.0796
Sand permeability(x_2)	0.3459>0.005	-0.9428	0.0000	9.0586
Major anisotropy(x_3)	0.0012<0.005	3.2399	0.0000	-19.8387
Minor anisotropy(x_4)	0.0000	-5.1932	0.0000	-13.1585
Percentage of magnesite(x_5)	0.0000	22.8311	0.0000	35.7136

5. CONCLUSIONS AND RECOMMENDATIONS

In this study, first using Petrel to simulation spatial distribution of magnesite and sand, then using Crunch Flow to simulate different spatial distribution of magnesite dissolution, final using regression models to analysis the correlation of the overall rate and the average porosity with different parameters: permeability of magnesite and sand, major anisotropy, minor anisotropy, percentage of magnesite and sand. At different parameter conditions, the correlation of the average porosity and the overall rate was slightly different. The following is a summary regression analysis of the data used in the thesis:

- Percentage of magnesite (or sand) is the most important parameter for both the average porosity and the overall rate. It has a positive correlation with them. And the percentage of magnesite correlation coefficient is greater than another parameter of about 10 times.
- The permeability of magnesite has a positive correlation with the overall rate and negative correlation with the average porosity, they are both weak correlation. For the overall rate, the weakest parameter is permeability of magnesite. The permeability of sand does not have a correlation with the overall rate. And for average porosity, it is negative correlation and a very weak parameter.
- Major anisotropy has a positive correlation with the overall rate and negative correlation with the average porosity; neither provides strong correlation. And in some special permeability, major anisotropy does not correlate with the overall rate.

- Minor anisotropy has both negative correlation with the overall rate and the average porosity. And in some special permeability, minor anisotropy also has non-correlation with the overall rate.

In total, the spatial distribution affects the average porosity and the overall rate. For this thesis, the percentage of magnesite (or sand) is the foremost parameter; next is the anisotropy (major and minor), and finally, we have the permeability (magnesite and sand).

BIBLIOGRAPHY

Alekseyev, V. A., et al. (1997). "Change in the dissolution rates of alkali feldspars as a result of secondary mineral precipitation and approach to equilibrium." Geochimica et Cosmochimica Acta 61(6): 1125-1142.

Bagheri, M. A. and A. T. Settari (2006). Modeling fluid flow in deformable fractured reservoirs using full tensor permeability. Golden Rocks 2006, The 41st US Symposium on Rock Mechanics (USRMS), American Rock Mechanics Association.

Bear, J. (2013). Dynamics of fluids in porous media, Courier Corporation.

Boguski, J. G. (1876). "Ueber die Geschwindigkeit der chemischen Vorgänge." Berichte der deutschen chemischen Gesellschaft 9(2): 1646-1652.

Bohling, G. (2005). "Introduction to geostatistics and variogram analysis." Kansas geological survey 2.

Brantley, S., et al. (2008). "Modelling chemical depletion profiles in regolith." Geoderma 145(3): 494-504.

Chou, L., et al. (1989). "Comparative study of the kinetics and mechanisms of dissolution of carbonate minerals." Chemical Geology 78(3): 269-282.

Darrouzet-Nardi, A. (2010). "Landscape heterogeneity of differently aged soil organic matter constituents at the forest-alpine tundra ecotone, Niwot Ridge, Colorado, USA." Arctic, Antarctic, and Alpine Research 42(2): 179-187.

Devidal, J.-L., et al. (1997). "An experimental study of kaolinite dissolution and precipitation kinetics as a function of chemical affinity and solution composition at 150 C, 40 bars, and pH 2, 6.8, and 7.8." Geochimica et Cosmochimica Acta 61(24): 5165-5186.

Draper, N. R., et al. (1966). Applied regression analysis, Wiley New York.

Faurholt, C. (1924). "Etudes sur les solutions aqueuses d'anhydride carbonique et d'acide carbonique." J Chim Phys 21: 400-455.

Fox, J. (1997). Applied regression analysis, linear models, and related methods, Sage Publications, Inc.

Gringarten, E. and C. V. Deutsch (2001). "Teacher's aide variogram interpretation and modeling." Mathematical Geology 33(4): 507-534.

Gronowitz, E., et al. (2006). "Serum phospholipid fatty acid pattern is associated with bone mineral density in children, but not adults, with cystic fibrosis." British journal of nutrition 95(06): 1159-1165.

Hair, J. F., et al. (2006). Multivariate data analysis, Pearson Prentice Hall Upper Saddle River, NJ.

Hamzaoui-Azaza, F., et al. (2011). "Hydrogeochemical characteristics and assessment of drinking water quality in Zeuss–Koutine aquifer, southeastern Tunisia." Environmental Monitoring and Assessment 174(1-4): 283-298.

Hewett, T. A. and R. A. Behrens (1990). "Conditional simulation of reservoir heterogeneity with fractals." SPE Formation Evaluation 5(03): 217-225.

Jackson, R. and M. Caldwell (1993). "The scale of nutrient heterogeneity around individual plants and its quantification with geostatistics." Ecology 74(2): 612-614.

Journel, A. G. and C. V. Deutsch (1998). GSLIB Geostatistical software library and users guide, Oxford University Press, New York.

Levenson, J. D. (2013). Sinai and zion, Harper Collins.

Li, L., et al. (2007). "Diversity enhances agricultural productivity via rhizosphere phosphorus facilitation on phosphorus-deficient soils." Proceedings of the National Academy of Sciences 104(27): 11192-11196.

Li, L., et al. (2007). "Applicability of averaged concentrations in determining geochemical reaction rates in heterogeneous porous media." American Journal of Science 307(10): 1146-1166.

Li, L., et al. (2014). "Spatial zonation limits magnesite dissolution in porous media." Geochimica et Cosmochimica Acta 126: 555-573.

Liu, Z. and W. Dreybrod (1997). "Dissolution kinetics of calcium carbonate minerals in H 2 O ・ CO 2 solutions in turbulent flow: The role of the diffusion boundary layer and the slow reaction H 2 O+ CO 2→ H++ HCO 3−." Geochimica et Cosmochimica Acta 61(14): 2879-2889.

Lüttge, A., et al. (2013). "A stochastic treatment of crystal dissolution kinetics." Elements 9(3): 183-188.

Lyuksyutov, I. F. and V. Pokrovsky (1998). "Magnetization controlled superconductivity in a film with magnetic dots." Physical review letters 81(11): 2344.

Maher, K. (2010). "The dependence of chemical weathering rates on fluid residence time." Earth and Planetary Science Letters 294(1): 101-110.

Manto, H. (2005). "Modelling of geometric anisotropic spatial variation." Mathematical Modelling and Analysis: 361-366.

Molins, S., et al. (2012). "An investigation of the effect of pore scale flow on average geochemical reaction rates using direct numerical simulation." Water Resources Research 48(3).

Mousavi-Avval, S. H., et al. (2011). "Energy flow modeling and sensitivity analysis of inputs for canola production in Iran." Journal of Cleaner Production 19(13): 1464-1470.

Murphy, D. J. and I. Cummins (1989). "Biosynthesis of seed storage products during embryogenesis in rapeseed, Brassica napus." Journal of plant physiology 135(1): 63-69.

Norusis, M. J. (2006). SPSS 15.0 guide to data analysis, Prentice Hall Upper Saddle River, NJ.

Nugent, M., et al. (1998). "The influence of natural mineral coatings on feldspar weathering." Nature 395(6702): 588-591.

Plummer, L., et al. (1978). "The kinetics of calcite dissolution in CO 2-water systems at 5 degrees to 60 degrees C and 0.0 to 1.0 atm CO 2." American Journal of Science 278(2): 179-216.

Plummer, L. N. and T. Wigley (1976). "The dissolution of calcite in CO2-saturated solutions at 25 C and 1 atmosphere total pressure." Geochimica et Cosmochimica Acta 40(2): 191-202.

Pokrovsky, O. (1998). "Precipitation of calcium and magnesium carbonates from homogeneous supersaturated solutions." Journal of Crystal Growth 186(1): 233-239.

Pokrovsky, O. S., et al. (1999). "Dolomite surface speciation and reactivity in aquatic systems." Geochimica et Cosmochimica Acta 63(19): 3133-3143.

Raza, N. and Z. I. Zafar (2013). "An Analytical Model Approach for the Dissolution Kinetics of Magnesite Ore Using Ascorbic Acid as Leaching Agent." International Journal of Metals 2013.

Reeves, D. and D. H. Rothman (2013). "Age dependence of mineral dissolution and precipitation rates." Global Biogeochemical Cycles 27(3): 906-919.

Salehikhoo, F., et al. (2013). "Magnesite dissolution rates at different spatial scales: The role of mineral spatial distribution and flow velocity." Geochimica et Cosmochimica Acta 108: 91-106.

Saltelli, A., et al. (2008). Global sensitivity analysis: the primer, John Wiley & Sons.

Schott, J., et al. (1989). "Dissolution kinetics of strained calcite." Geochimica et Cosmochimica Acta 53(2): 373-382.

Sjöberg, E. L. and D. T. Rickard (1984). "Temperature dependence of calcite dissolution kinetics between 1 and 62 C at pH 2.7 to 8.4 in aqueous solutions." Geochimica et Cosmochimica Acta 48(3): 485-493.

Smith, J., et al. (2005). "Projected changes in mineral soil carbon of European croplands and grasslands, 1990–2080." Global Change Biology 11(12): 2141-2152.

Steefel, C. (2009). "CrunchFlow software for modeling multicomponent reactive flow and transport. User's manual." Earth Sciences Division. Lawrence Berkeley, National Laboratory, Berkeley, CA. October: 12-91.

Steefel, C. I. and A. C. Lasaga (1994). "A coupled model for transport of multiple chemical species and kinetic precipitation/dissolution reactions with application to reactive flow in single phase hydrothermal systems." American Journal of Science 294(5): 529-592.

Swoboda-Colberg, N. G. and J. I. Drever (1993). "Mineral dissolution rates in plot-scale field and laboratory experiments." Chemical Geology 105(1): 51-69.

Wackernagel, H. (2013). Multivariate geostatistics: an introduction with applications, Springer Science & Business Media.

Wagner, H. M. (1995). "Global sensitivity analysis." Operations Research 43(6): 948-969.

Warrick, A. and D. Myers (1987). "Optimization of sampling locations for variogram calculations." Water Resources Research 23(3): 496-500.

Webster, R. and M. Oliver (1993). How large a sample is needed to estimate the regional variogram adequately? Geostatistics Tróia'92, Springer: 155-166.

White, A. F. and S. L. Brantley (2003). "The effect of time on the weathering of silicate minerals: why do weathering rates differ in the laboratory and field?" Chemical Geology 202(3): 479-506.

Wollast, R. (1990). "Rate and mechanism of dissolution of carbonates in the system CaCO 3-MgCO 3." IN: Aquatic Chemical Kinetics: Reaction Rates of Processes in Natural Waters. Environmental Science and Technology Series. John Wiley & Sons, New York. 1990. p 431-445. 6 Figure, 1 tab, 26 ref.

Zhu, Y., et al. (2011). "Carbon-based supercapacitors produced by activation of graphene." Science 332(6037): 1537-1541.

VITA

Yao Wang received her Bachelor of Science degree in geology and geophysics from Missouri University of Science and Technology in May 2014, and she received Bachelor of Science degree in geology engineering from China University of Petroleum in June 2014. She started to pursue her master degree at Petroleum Engineering department of Missouri University of Science and Technology in August 2014. She joined Dr. Heidari's group from March 2015. In December 2016, she received her Master's Degree in Petroleum Engineering from Missouri University of Science and Technology.